A COMMUNICATION ANALYSIS OF HIGH-FREQUENCY IONOSPHERIC SCATTERING

GÖRAN EINARSSON

TECHNICAL REPORT 400

NOVEMBER 15, 1962

MASSACHUSETTS INSTITUTE OF TECHNOLOGY
RESEARCH LABORATORY OF ELECTRONICS
CAMBRIDGE, MASSACHUSETTS

The Research Laboratory of Electronics is an interdepartmental laboratory in which faculty members and graduate students from numerous academic departments conduct research.

The research reported in this document was made possible in part by support extended the Massachusetts Institute of Technology, Research Laboratory of Electronics, jointly by the U.S. Army (Signal Corps), the U.S. Navy (Office of Naval Research), and the U.S. Air Force (Office of Scientific Research) under Signal Corps Contract DA 36-039-sc-78108, Department of the Army Task 3-99-20-001 and Project 3-99-00-000; and in part by Signal Corps Contract DA-SIG-36-039-61-G14.

MASSACHUSETTS INSTITUTE OF TECHNOLOGY

RESEARCH LABORATORY OF ELECTRONICS

Technical Report 400 November 15, 1962

A COMMUNICATION ANALYSIS OF HIGH-FREQUENCY IONOSPHERIC SCATTERING

Göran Einarsson

Submitted to the Department of Electrical Engineering, M. I. T., January 15, 1962, in partial fulfillment of the requirements for the degree of Master of Science.

(Manuscript received March 15, 1962)

Abstract

A communication scheme for random multipath channels is investigated. During predetermined intervals the transmitter sends a sounding signal that the receiver uses to predict the behavior of the channel during the intermediate time when communication is performed. It is assumed that the channel varies slowly, and that the additive noise in the receiver is low.

The possibility of representing a multipath channel as a time-variant filter is investigated. A sampling theorem for linear bandpass filters is derived, and the results that can be expected when it is used to represent a single fluctuating path with Doppler shift are discussed.

The prediction operation is essentially linear extrapolation: a formula for the mean-square error is derived and compared with optimum linear prediction in a few cases. Calculations on actual data from ionospheric scattering communication show that the method is feasible and give good correspondence with the theoretical results.

Under the assumption that the receiver makes decisions on each received waveform separately, and that there is no overlap between successive waveforms, the optimum receiver is derived. It consists mainly of a set of matched filters, one for each of the possible waveforms. The predicted value of the channel parameters is used in weighting the output from the matched filters to obtain likelihood ratios.

The eventual practical value of such a communication system is still an open question, but this formulation provides means for dealing with random multipath channels in a way suitable for mathematical analysis.

TABLE OF CONTENTS

CONTENTS

I. INTRODUCTION

1.1 HISTORY OF THE PROBLEM

a. The Probability Computing Receiver

The problem of detecting known signals disturbed by additive noise can be stated as follows (see Fig. 1). The transmitter has M possible waveforms, each of duration T. It sends one of them, say $\xi_k(t)$ with probability P(k). The signal is disturbed by additive white Gaussian noise $\eta(t)$ and the received signal is $\zeta_k(t) = \xi_k(t) + \eta(t)$. We assume that the receiver knows the form of the M possible waveforms and we want it to determine which one was sent. All of the information that the receiver needs for that purpose is contained in the set of a posteriori probabilities $P(\xi_k(t)/\zeta(t))$, $k = 1, \ldots, M$. It is clear that a receiver that computes this for all k and chooses the index which gives the largest probability minimizes the probability of making a mistake. Using Bayes' equality we can write

$$P(\xi_k(t)/\zeta(t)) = \frac{P(k)\, p(\zeta(t)/\xi_k(t))}{\sum_{\nu=1}^{M} P(\nu)\, p(\zeta(t)/\xi_\nu(t))} \tag{1}$$

where p denotes probability density. Since the denominator of (1) is a constant independent of the index k and the P(k) was assumed to be known, the receiver need only compute the conditional probability density $p(\zeta(t)/\xi_k(t))$ for each k. Since the noise is Gaussian, $p(\zeta(t)/\xi_k(t))$ is going to be a Gaussian density and it is possible to show that

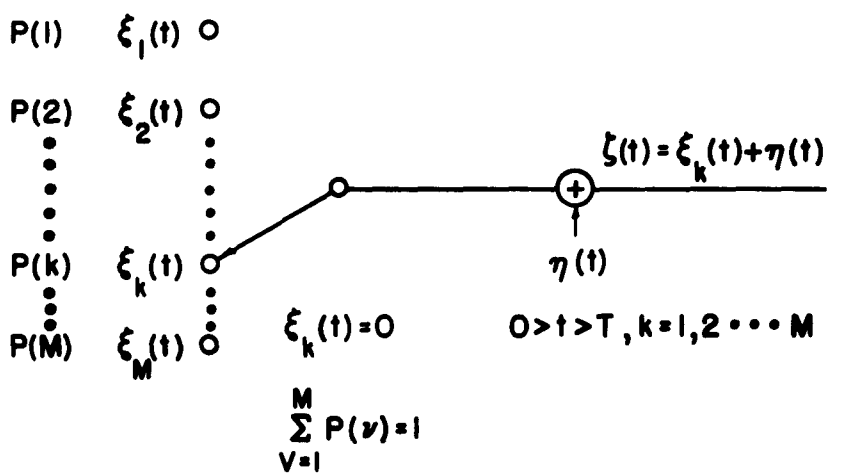

Fig. 1. Signals disturbed by white Gaussian noise.

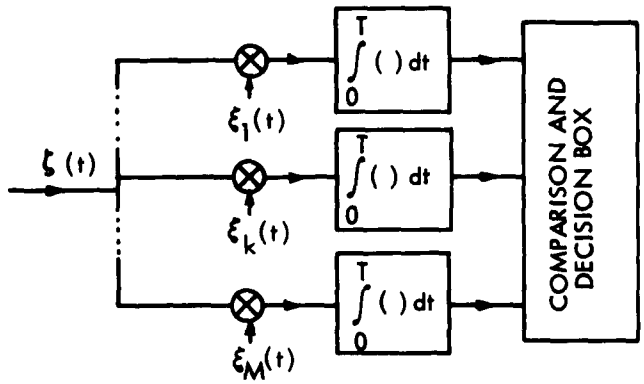

Fig. 2. Optimum receiver for additive white Gaussian noise.

$$p(\zeta(t)/\xi_k(t)) = \text{const.}\ e^{\frac{2T}{N_o}(\rho_k - 1/2\ S_{kk})} \tag{2}$$

where

$$\rho_k = \frac{1}{T}\int_0^T \xi_k(t)\ \zeta(t)\ dt \tag{3}$$

$$S_{kk} = \frac{1}{T}\int_0^T \xi_k^2(t)\ dt \tag{4}$$

and N_o is the noise power per unit bandwidth. We see that the receiver has to evaluate the correlation integral ρ_k between the received waveform and each possible transmitted waveform. This can be done, for instance, by matched filters. The receiver then takes into account the possible difference in signal energy and signal probabilities, P(k), and decides which waveform was actually sent. (See Fig. 2.)

The receiver of Fig. 2 performs these desired operations; in this report we use the term "optimum receiver" for a device that computes the probability density $p(\zeta(t)/\xi_k(t))$ or a monotonically related function in order to make its decision. We have stated the problem as a one-shot problem but for white Gaussian noise it is clear that the performance of the receiver is still optimum whenever the transmitted waveforms are statistically independent of each other. A more detailed presentation of the optimum receiver for additive noise has been given by Fano.[9]

Let us now consider a more general problem in which the transmitted signal is perturbed by a random channel in addition to the white noise. (See Fig. 3.) By the term random channel, we mean a linear time varying filter whose variation is guided, in general, by a multidimensional random process. The problem of determining the function of the probability computing receiver in this case has been studied by several authors. In the next paragraph we review some of the results obtained.

b. Other Research

We shall discuss some of the results for the optimum receiver for the general case illustrated by Fig. 3, obtained by Price,[16] Turin,[21] and Kailath.[11] Their approaches differ mainly in the class of random channels considered. Price and Turin deal with ionospheric-scattering communication and work with channels that have multipath

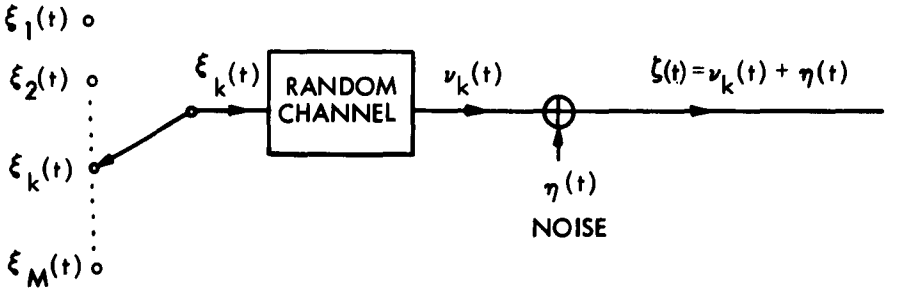

Fig. 3. Signals disturbed by a random channel plus noise.

structure. Kailath considers a very general channel for which the statistics need not even be stationary. All three authors assume that the receiver has complete knowledge about the statistics of the channel and the additive noise, which are assumed to be statistically independent of each other. The decision is made on each waveform separately. This means that the receiver is, strictly speaking, optimum only for the "one-shot case," since it does not exploit the fact that successive output waveforms may be statistically dependent. Finally, it is assumed that both the transmitter and the receiver have the same time standard.

Price considers a random channel that consists of a number of paths with known delay. Each path has a stationary narrow-band Gaussian process associated with it. The different paths are assumed to be statistically independent. If we send an unmodulated carrier through this channel, we receive $Z(t) = y_c(t) \cos \omega_o t - y_s(t) \sin \omega_o t$, where $y_c(t)$ and $y_s(t)$ are lowpass, independent, Gaussian processes with zero mean and identical autocorrelation. The first-order statistics of the envelope of $Z(t)$ are then Rayleigh distributed and the phase distribution is flat. See, for instance, Davenport and Root[7] for a presentation of the narrow-band Gaussian process. For this type of channel, Price obtains the optimum receiver in open form. The operations that the receiver should perform are given in the form of integral equations. For the special case of a single path and input signals that are constant or vary exponentially with time, they derive in detail the structure of the probability computing elements. The case of very low signal-to-noise ratio is also considered in some detail.

Turin works with a similar multipath model. The channel is represented by a number of independent paths each of which is characterized by a path-strength a_i, a phase

shift θ_i, and a delay τ_i. The channel is so slowly varying that these quantities can be considered as constants during the transmission time T. The strength and phase shift of the paths are assumed to be represented by a constant vector plus a vector with Rayleigh distribution for amplitude and completely random phase. Since the Rayleigh distribution is characterized by a single parameter, say σ_i, each path is determined by four quantities: the amplitude a_i and the phase δ_i of the constant vector and σ_i and τ_i. For the case $a_i = 0$, Turin's channel is the same as Price's for slowly varying paths. Turin considered the following cases: the receiver knows all four channel parameters; the receiver does not know δ (in which case it assumes completely random phase); τ and δ are not known and the receiver assumes δ to be completely random and τ to have a flat distribution within two time limits. It is interesting to notice that the optimum receiver under most of the conditions above computes the correlation integral between the received signal and the possible transmitted signals delayed according to the path delay τ_i. The terms corresponding to different paths are then combined, by using the known statistical parameters of the paths, to obtain the probabilities $p(\zeta(t)/\xi_k(t))$.

Kailath has a much more general random channel than Price and Turin. His only restriction is that the channel be Gaussian, i. e., that the output $\nu_k(t)$ sampled at arbitrary instants of time gives a multidimensional Gaussian distribution for all values of k. When $\nu_k(t)$ has zero mean for all t, Kailath derives an optimum receiver that looks like Fig. 4. He shows, also, that the estimating filters H_k can be interpreted as a mean-square-error estimator of $\nu_k(t)$ when k was actually sent. The same result was obtained earlier by Price for the random filter consisting of a single path. We see that when the receiver does not know the channel exactly, it estimates, on the basis of its statistical knowledge, what the received signal should look like before the noise was added if a particular signal was sent. It then crosscorrelates this estimate with the actually received signal to obtain a quantity that is monotonically related to the a posteriori probabilities

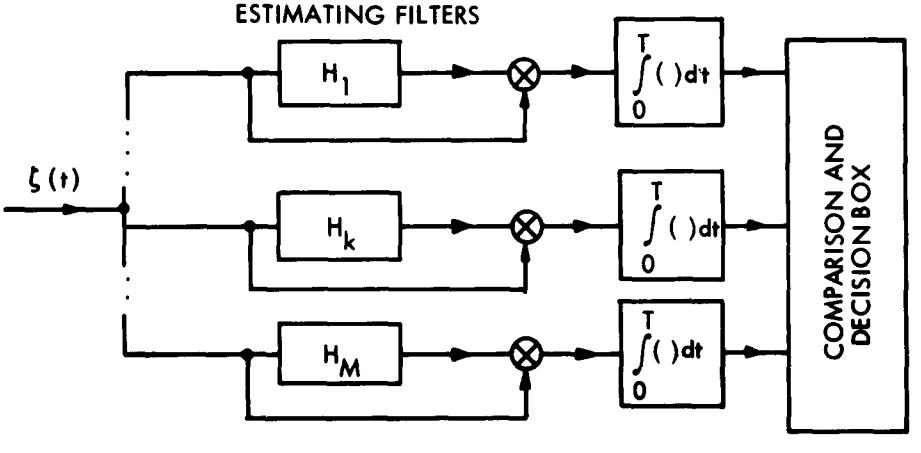

Fig. 4. Optimum receiver for zero mean Gaussian random channel plus noise.

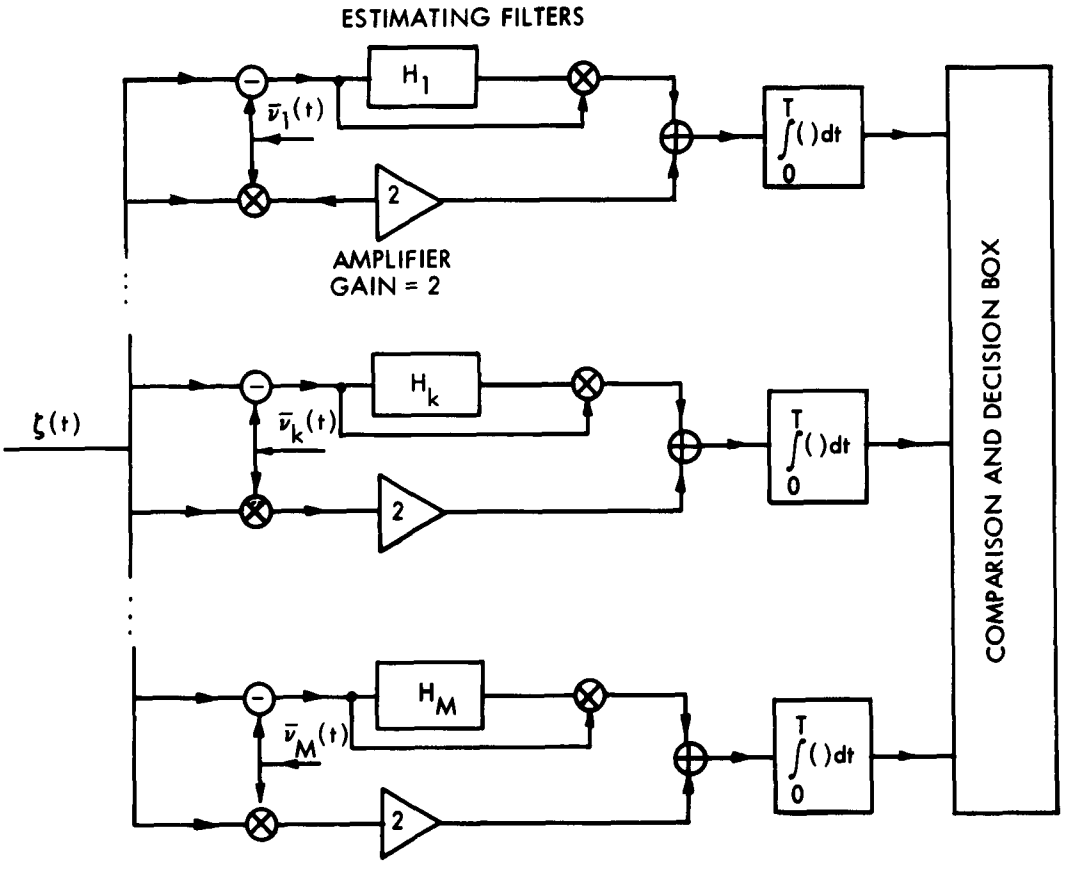

Fig. 5. Optimum receiver for Gaussian random channel plus noise (General Case).

It is important to notice that this interpretation of the optimum receiver is valid only if $\nu_k(t)$ has zero mean. When this is not the case, Kailath gives the receiver structure of Fig. 5 in which $\bar{\nu}_k(t)$ is the mean of $\nu_k(t)$ (already known by the receiver under the assumption that a particular k was used). The gain factor 2 on the amplifier shows that the receiver puts greater weight on the part of the signal that it knows exactly than on the part it has to estimate.

Kailath considers a very general case and he obtains very general results. His estimating filters are given in the form of limits of very large inverted matrices. It is hard to say much more than that it is possible to instrument them as linear time-variant filters.

c. Discussion

Price and Turin consider specific multipath models that are more or less applicable to ionospheric-scattering communication, while Kailath considers a more general model. The thing that they have in common is the assumption that the receiver has complete

statistical knowledge of the channel. To obtain this statistical knowledge, we have to measure the parameters of the channel, but since additive noise is present, we cannot do this exactly. To build an estimator that is optimum in some sense, we need to know in advance some of the statistical parameters that we want to measure. To some extent this is a closed circle, but we can, at least in principle, start guessing the statistical parameters that we need and then construct an optimum estimator on the basis of this guess. This, we hope, gives us a better estimate of the statistics and we can use this as a priori information to construct a better estimator, and so on.

Perhaps a more serious problem to consider is whether or not the channel is stationary. For a statistical description to be at all useful, the channel has to be at least quasi-stationary; that is, we can consider it stationary during the time in which we are using it for communication. If the properties of the channel change and we have to make repetitive measurements of the statistical parameters and then change our optimum receiver according to these measurements, we have a painfully elaborate scheme.

As we have pointed out, the theoretical work on optimum receivers has been done under the assumption that the receiver makes its decision on each waveform separately. If the channel is varying very fast, so that the disturbances from one transmitted signal to the next are essentially independent, this is clearly the best that we can do. If, on the other hand, the channel changes only slowly during the transmission of a signal, we are not using all of the available information about the channel. Since the receiver tries to circumvent the fact that it does not know exactly what the channel was by making an estimate on the basis of the received waveform, it can clearly do better in the case of slow variations by extending this estimate over consecutive signals.

The RAKE receiver described by Price and Green[17] is an attempt to use the ideas of optimum receivers for combatting random multipath in a practical case. Two orthogonal waveforms are used, and the receiver makes an estimate of the path structure of the channel by crosscorrelating the sum of the two possible signals with the received signal. It is possible to do this, since the signals have nonoverlapping spectra. The time constant of the correlator is greater than the duration of the signal, and the receiver is thus operating over more than one signal at a time. The estimate of the path structure is then used to correct the received signal before the decision is made.

If the channel is nonstationary and the receiver is faced with the problem of obtaining statistical knowledge of the channel, it is perhaps just as easy for the receiver to try to measure the channel itself. For such measurements to be useful, the channel must vary slowly, so that it does not change much between transmitted signals. Price[15] and Turin[20] have discussed the possibility of estimating the instantaneous state of the channel by using a sounding waveform known to the receiver. In this report we are going to outline a communication procedure that is based on this idea for a slowly varying multipath medium.

1.2 THE IONOSPHERE

The propagation of radio waves via ionized layers in the upper atmosphere has been considered for more than half a century and an established theory exists. For a certain incident angle there is a maximum usable frequency (MUF) below which the wave is returned to earth by a process of gradual refraction. Since there exist several layers at different altitudes and, in addition, the wave can make several hops, it is clear that we are dealing with a multipath medium. Other things that contribute to this structure are the splitting of the wave into an ordinary wave and an extraordinary wave because of the earth's magnetic field, and the possibility of a ground wave. The mathematical theory of radio waves in the ionosphere can be found in Budden.[6]

A different kind of propagation mode, called scattering, has received considerable attention during the last decade. If there are irregularities in the ionosphere, they act as oscillating electric dipoles when exposed to an electromagnetic wave, and in this way energy can return to the earth. The possibility of using scattering for long distance communication was pointed out in a paper by Bailey and others.[1] The scattered field is comparatively weak, but it provides means for communication beyond the horizon with frequencies higher than the MUF.

In a paper written in 1948, Ratcliffe[18] pointed out that if we assume that the downcoming wave is scattered by many "scattering centra," each scattering the same amount of power and completely randomly distributed in space, we are going to receive a narrow-band Gaussian process if we send up an unmodulated carrier. Moreover, if the scattering centra move in the same fashion as molecules in a gas, that is, if the line-of-sight velocity has a Gaussian distribution, the power spectral density of the downcoming wave is Gaussian and of the form

$$W(f) = \frac{1}{\sigma\sqrt{2\pi}} e^{-(f-f_o)^2/2\sigma^2}, \tag{5}$$

where

$$\sigma = \frac{2f_o V_o}{c},$$

with V_o the rms velocity of the scattering centra, and f_o the frequency of the incident wave. We can state these properties in another way. The downcoming wave can be expressed in the form

$$Z(t) = V(t) \cos (2\pi f_o t + \phi(t)). \tag{6}$$

The envelope V(t) has a Rayleigh distribution of the form

$$p(V_t) = \frac{V_t}{\sigma^2} e^{-\frac{V_t^2}{2\sigma^2}} \qquad V_t \geq 0 \tag{7}$$

If we look at the quadrature components

$$y_s(t) = V(t) \sin \phi(t) \quad \text{and} \quad y_c(t) = V(t) \cos \phi(t)$$

we see that they are independent Gaussian processes with identical autocorrelation of Gaussian form.

We notice that these statistics correspond to the assumptions in Price's work about the optimum receiver.

If, in this idealized case, we have a specular component of amplitude A in the downcoming wave, the distribution for the envelope takes the form

$$p(V_t) = \frac{V_t}{\sigma^2} e^{-\frac{V_t^2+A^2}{2\sigma^2}} I_o\left(\frac{AV_t}{\sigma^2}\right) \qquad V_t \geq 0 \tag{8}$$

See Davenport and Root[7] for a derivation. This kind of distribution was first considered by Rice[19] in his classical paper of 1945, and we use the name "Rician distribution" for it. This was the type of statistics which Turin used in his work.

Ratcliffe's model of the scattering process is, of course, too simple to represent the physical phenomena that occur. More complicated theories have been presented by Booker and Gordon,[3] Villars and Weisskopf,[23] and others, but they all seem to lead to the Rayleigh distribution for the envelope when there is no specular component.

Measurements of the statistics of scattered radio waves have been presented by many authors. A brilliant and extensive study of ionospheric transmission at medium frequency (543 kcps) has been made by Brennan and Phillips.[4] They computed the distribution of the envelope of the received wave and made a test to determine whether or not it had a Rician or Rayleigh distribution. The result was perhaps somewhat disappointing; in more than half of the 200, or more, cases analyzed, they determined "no fit." The computed correlation functions for the envelope took many widely different forms, and it was not possible to assign any general shape to them.

The ionospheric scattering has multipath structure if we have different scattering regions with different transmission times. Most of the measurements reported have been made with a continuous wave, and very little is known about the statistics of the multipath structure. It should be of interest to know, among other things, more about how many paths are present, if the paths are statistically independent, and the nature of variation in the delay between paths. Another effect that needs to be studied is the Doppler effect that a steadily moving scattering region should produce. Some work in this area is presented in a thesis by Pratt,[16] and other work is being done at Lincoln Laboratory, M. I. T.

1.3 THE COMMUNICATION SYSTEM TO BE CONSIDERED

On the basis of the theoretical investigations that have been reviewed we are going to outline a possible scheme for communication over random multipath channels. The

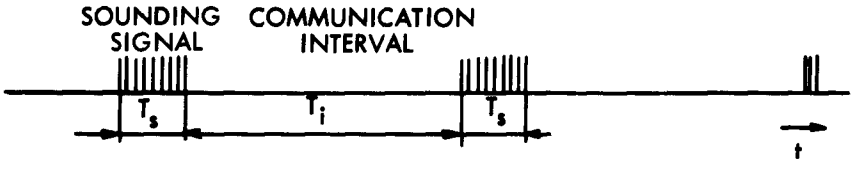

Fig. 6. Transmitted signals

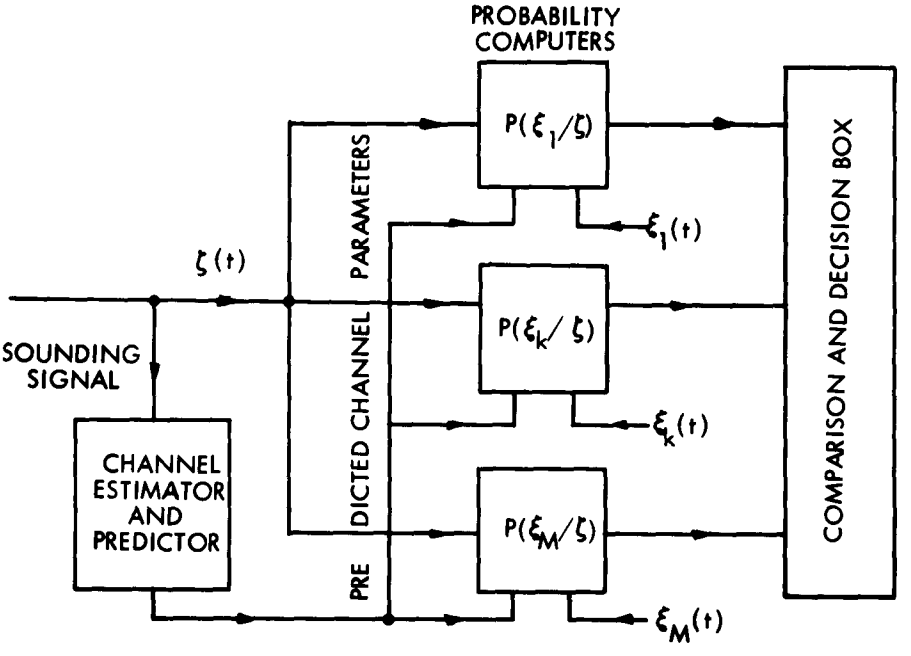

Fig. 7. Receiver structure.

receiver is probably not optimum in any sense, but it should work well, at least, under certain conditions.

We assume that the transmitter sends information during the time intervals of length T_i. Between these intervals, it sends a predetermined signal of length T_s from which the receiver tries to obtain knowledge about the multipath medium. In the particular case considered here, this sounding signal consists of a number of short pulses; with these as a basis the receiver tries to predict the behavior of certain channel parameters during the next T_i seconds. The receiver uses this predicted knowledge about the channel when it makes its decision of what was sent. See Figs. 6 and 7.

The prediction operation that is to be used is simply linear extrapolation. See Fig. 8. During the T_s seconds the receiver knows that channel parameter exactly apart from additive noise. It determines a straight line that fits the curve in a least-square sense, and uses this line as predicted value of the parameter for the next T_i seconds, during

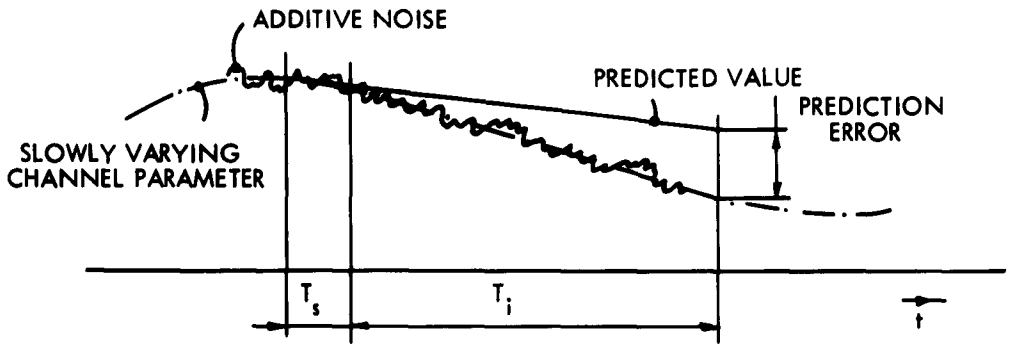

Fig. 8. Prediction operation.

which information is being sent. This procedure contains a smoothing operation that is necessary because of the additive noise, but does not use any statistical knowledge about the process and it should work just as well (or badly) in a nonstationary case as in a stationary one.

This procedure is clearly based on some assumptions: that it is possible to characterize the multipath medium with a number of slowly varying parameters; that the signal-to-noise ratio is high enough, and so on. Measurements made by Group 34 at Lincoln Laboratory seem to indicate that it should be possible to use the outlined procedure for ionospheric scattering HF communication, and we are going to investigate it for that kind of channel.

We first consider the problem of representing the ionospheric scattering with a model channel whose parameters are simple to measure and predict, and which is still capable of representing the channel closely enough for practical purposes. Section II deals with the prediction operation and some calculations are carried out with actual ionospheric data. In Section IV the derivation of the receiver structure is given.

II. A MODEL OF SCATTERING MULTIPATH

2.1 INTRODUCTION

To work our problem we need a model of the communication channel. First, we consider the representation of ionospheric scattering by a time-variant linear network. The assumption that the receiver makes repetitive measurements of the channel emphasizes the need for a simple model with a limited number of parameters to be determined. The linear-network approach has the advantage of being quite general, but it seems to lead to unnecessary complexity when it is used to represent multipath or frequency shift. The model that we chose to use is discussed in the last part of this Section and it is based mainly on physical facts about scattering communication.

2.2 LINEAR NETWORK REPRESENTATION

a. Sampling Theorem and Delay-Line Model

If we consider a communication link having wave propagation in a time-variant but linear medium, we can characterize the channel as a filter with an impulse response changing with time. See Fig. 9. The response function h(y, t) contains all information about the channel that we can possibly need, but it can be extremely complicated. For electromagnetic wave propagation, for instance, with signals of different frequencies traveling according to different physical mechanisms, it would be hard to visualize any over-all impulse response. In a practical case, in general, we use bandlimited signals in a narrow region, and we are not interested in such a complete description a knowledge of h(y, t) should provide. If our transmitted signal u(t) is bandlimited in the band $f_c - \frac{W}{2} \leq f \leq f_c + \frac{W}{2}$ it can be shown that (see Appendix A) that we can write the received signal as

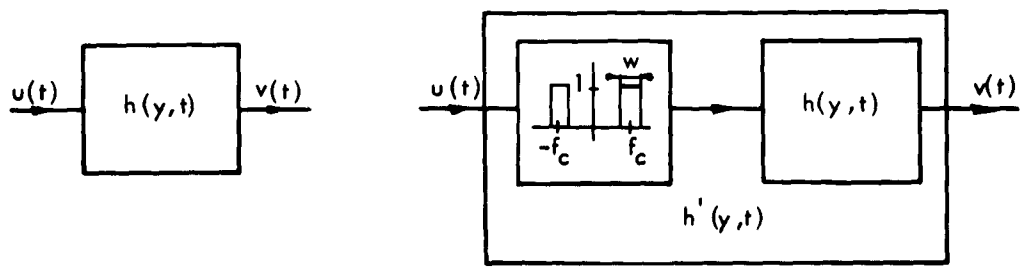

$$v(t) = \int_{-\infty}^{\infty} h(y,t)\,u(t-y)\,dy$$

$$v(t) = \int_{-\infty}^{\infty} h'(y,t)\,u(t-y)\,dy$$

$u(t)$ BANDLIMITTED: $f_c - \frac{W}{2} \leq |f| \leq f_c + \frac{W}{2}$

Fig. 9. Time-variant linear filter.

$$v(t) = \sum_n \frac{1}{2w}\, h'\left(\frac{n}{w}, t\right)\, u\left(t-\frac{n}{w}\right) - \sum_n \frac{1}{2w}\, \hat{h}'\left(\frac{n}{w}, t\right)\, \hat{u}\left(t-\frac{n}{w}\right), \tag{9}$$

where the circumflex denotes Hilbert transforms, and h'(y, t) is related to h(y, t) by the formula A-6 of Appendix A. If our signal u(t) is narrow-band (i.e., $f_c \gg w$), we can get an easy expression for the Hilbert transform.

Write u(t) in terms of its quadrature components

$$u(t) = u_c(t) \cos 2\pi f_c t - u_s(t) \sin 2\pi f_c t. \tag{10}$$

Taking the Hilbert transform (for instance, by passing it through the filter in Fig. A-2), we get

$$\hat{u}(t) = u_c(t) \sin 2\pi f_c t + u_s(t) \cos 2\pi f_c t. \tag{11}$$

Since $u_c(t)$ and $u_s(t)$ are slowly varying lowpass functions, we have

$$\hat{u}(t) \cong u\left(t - \frac{1}{4f_c}\right),$$

and analogously $\hat{h}'(y, t) \cong h'\left(y - \frac{1}{4f_c}, t\right)$.

The summations in Eq. 9 go from $-\infty$ to $+\infty$, but in most practical cases $h'\left(\frac{n}{w}, t\right)$ goes to zero rapidly enough for $|n|$ large, so we can introduce a suitable delay τ and represent formula (9) by the delay line in Fig. 10.

It should be pointed out that the particular form of the response function for the time-variant network that we have chosen is not the only possible one. Our treatment of the

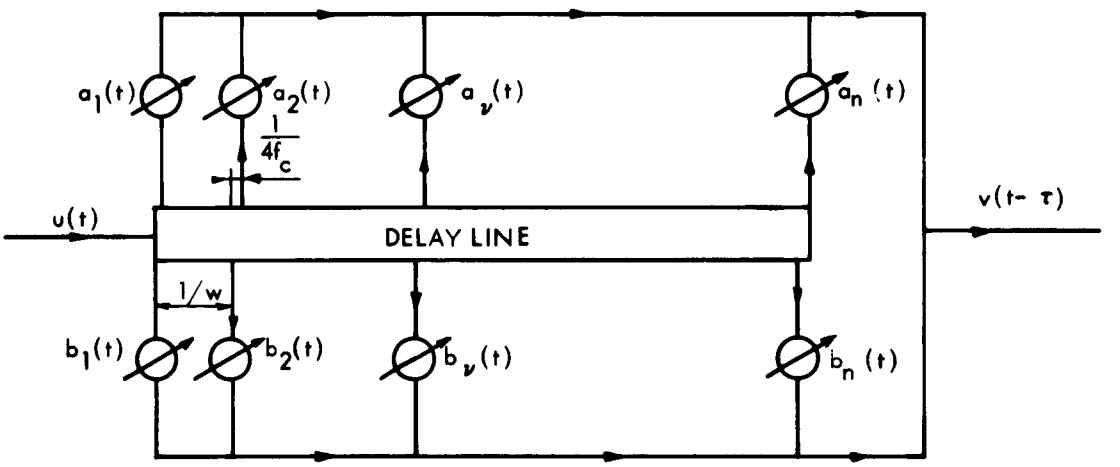

$$a_\nu(t) = \frac{1}{2w}\, h'\left(\frac{\nu}{w}, t\right) \quad ; \quad b_\nu(t) = \frac{1}{2w}\, h'\left(\frac{\nu}{w} - \frac{1}{4f_c}, t\right)$$

Fig. 10. Delay-line model for narrow-band functions.

subject is very similar to that of Kailath[12] to which we refer for other possible representations.

b. Example 1

As an example we derive the delay-line model for the simple channel in Fig. 11, composed of a time delay δ and a frequency shift Δf. As is shown in Appendix A, we obtain

$$h'(y,t) = A2w \text{ sinc } [w(y-\delta)] \cos [2\pi(f_c(y-\delta)+\Delta ft)+\phi] \tag{12}$$

$$\hat{h}'(y,t) = A2w \text{ sinc } [w(y-\delta)] \sin [2\pi(f_c(y-\delta)+\Delta ft)+\phi] \tag{13}$$

If we choose f_c and w so that $f_c = NW$, where N is an integer, the tap gains in Fig. 10 become

$$a_\nu(t) = \frac{1}{2w} h'\left(\frac{\nu}{w}, t\right) = A \text{ sinc } \left(\nu - \frac{\delta}{w}\right) \cos (2\pi\Delta ft+\theta) \tag{14}$$

$$b_\nu(t) = \frac{1}{2w} \hat{h}'\left(\frac{\nu}{w}, t\right) = A \text{ sinc } \left(\nu - \frac{\delta}{w}\right) \sin (2\pi\Delta ft+\theta). \tag{15}$$

Here, $\theta = \phi + 2\pi f_c \delta$. The tap gain functions are simple sinusoids with frequency given by the frequency shift. The magnitude of a_ν or b_ν as a function of the tap number ν is given in Fig. 12 for $\delta = \frac{1}{2w}$.

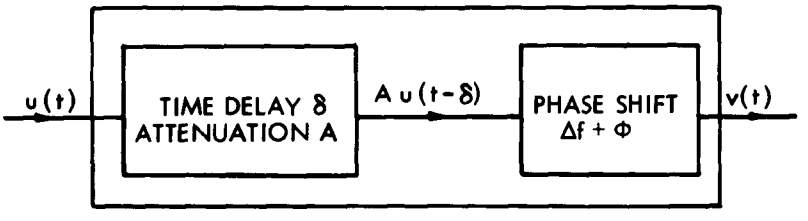

$$H(jf,t) = A\, e^{-j2\pi f\delta} \begin{cases} e^{j(2\pi\Delta ft+\Phi)} & f>o \\ e^{-j(2\pi\Delta ft+\Phi)} & f<o \end{cases}$$

Fig. 11. Filter with delay and frequency shift.

c. The ionosphere as a tapped delay line

Measurements of ionospheric radio-wave propagation indicate that the ionosphere can be considered a linear medium, at least in the sense that nonlinear effects are of second order. For communication purposes, the signal bandwidth is always much smaller than the carrier frequency. It should therefore be possible to represent the

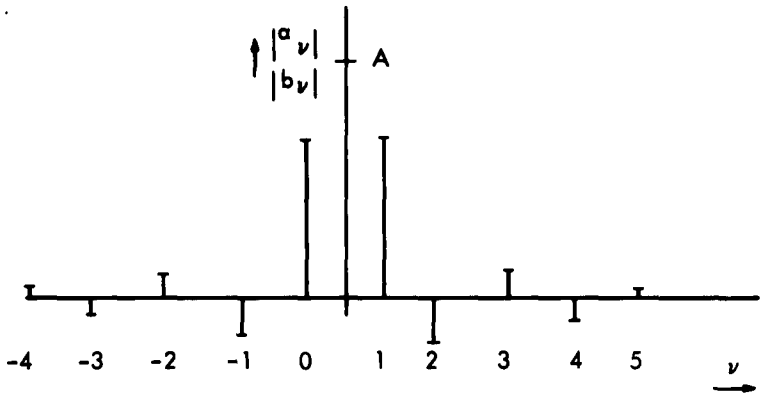

Fig. 12. Amplitude of the tap gain functions for the filter illustrated in Fig. 11.

ionosphere over a certain frequency band with the tapped delay line shown in Fig. 10.

If we decide to use the delay-line model, the question arises whether or not we can easily measure the tap gain functions. To determine the response function of a time-variant filter, we need to know the output signal corresponding to a number of succeeding input signals. This is difficult to perform for an ionospheric propagation link, since it is hard to establish the same time scale at both transmitter and receiver. The sampling theorem in formula (9) is in terms of samples of a high-frequency waveform. In practice it is inconvenient to instrument this directly, and some kind of demodulator is generally used in the measurement system.

Taking these matters into consideration, we investigate a particular way of measuring the characteristics of the ionosphere. We are interested in the frequency band $f_c - \frac{W}{2} \leq f \leq f_c + \frac{W}{2}$. As a sounding signal we use a lowpass function g(t) with a bandwidth $w_g \geq \frac{W}{2}$ and multiply it by a carrier frequency to get a narrow-band function. At the receiver we use a quadrature demodulator to provide information about the phase, as well as the amplitude of the received signal. We assume that the receiver knows the time at the transmitter apart from a constant value δ_ϵ and that the local oscillator in the demodulator is timed to the frequency $f_c + \Delta f_\epsilon$. See Fig. 13.

To get a feeling for what we can expect if we perform such measurements, let us consider replacing the ionosphere by the filter in Fig. 12, except that A and ϕ are slowly varying with time $\left(\text{slowly compared with } \frac{1}{W}\right)$ to get a fading effect. We can consider this as a model of a slowly varying path with Doppler shift. We send a sequence of g(t):s, spaced T seconds apart, and record the corresponding output from the demodulator. Since the parameters A and ϕ are slowly varying, we can use the results from Example 1, and the tap gains that we determine are of the form

$$a_\nu(t) = a_\nu A(t) \cos [2\pi\Delta ft + \theta(t)]$$

$$b_\nu(t) = b_\nu A(t) \sin [2\pi\Delta ft + \theta(t)]. \qquad (16)$$

With the simple channel structure that we have assumed, the outputs from the demodulator u_s and u_c are copies of g(t), spaced T seconds apart, but with varying amplitude. (See Fig. 13.) If we determine the amplitude for each transmission, the outputs can

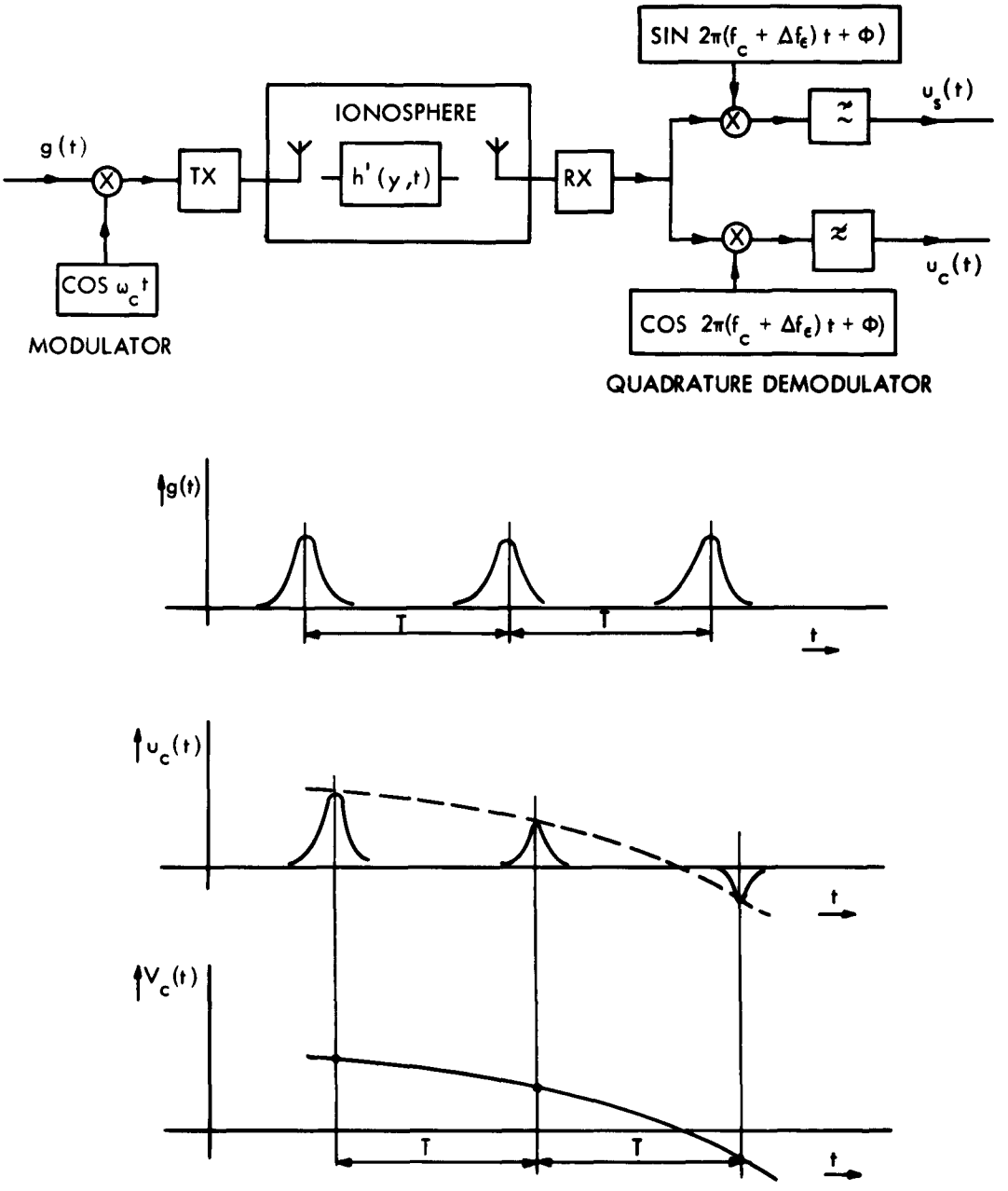

Fig. 13. Measurements of the ionosphere.

be considered as samples, t seconds apart, of the time functions

$$V_c(t) = A(t-\tau_\epsilon) \cos [(2\pi(\Delta f+\Delta f_\epsilon)(t-\tau_\epsilon)+\theta(t-\tau_\epsilon)] \tag{17}$$

$$V_s(t) = A(t-\tau_\epsilon) \sin [(2\pi(\Delta f+\Delta f_\epsilon)(t-\tau_\epsilon)+\theta(t-\tau_\epsilon)]. \tag{18}$$

It is thus possible to determine the tap gain functions apart from a time delay τ_ϵ and a frequency Δf_ϵ. If we use the same demodulator both for measurements and as a part of a receiver for communication, it is meaningless to distinguish between the uncertainties caused by the ionosphere or by the receiver and we can extend the model to include the particular receiver that we are using.

For a time-variant channel of more complex structure than we have considered, we can still obtain the tap gains by comparing the received signal with the transmitted. This is under the assumption that the time variation in the filter is slow enough so that the tap gains are determined by samples T seconds apart.

Example 1 tells us that, depending on Doppler effect in the channel or frequency deviations in the local oscillator of the receiver, the tap gain functions are of the form

$$a_\nu(t) = a_\nu(t) \cos (\Delta\omega_\nu t+\theta_\nu(t)) \tag{19}$$

for a slowly varying path.

d. Modulated Random Processes

If we apply a statistical description to our time-variant channel, the tap gain functions of the delay-line model are sample functions of random processes. To gain some insight into what kind of processes we can expect, let us substitute the single path filter of Fig. 11 for the ionosphere and assume that we know the statistical properties of A(t) and $\phi(t)$ (with Δf assumed constant).

We define two new functions

$$x_s(t) = A(t) \sin \phi(t) \tag{20}$$

$$x_c(t) = A(t) \cos \phi(t). \tag{21}$$

We can determine the tap gain functions apart from an uncertainty of time origin, and we have

$$a_\nu(t) = a_\nu A(t) \cos (\Delta\omega t+\phi(t)+\psi) \tag{22}$$

$$b_\nu(t) = a_\nu A(t) \sin (\Delta\omega t+\phi(t)+\psi), \tag{23}$$

Here, $\Delta\omega$ is considered as a constant and is caused by the Doppler shift of the path and the frequency error of the local oscillator in the receiver. The constant phase angle ψ is due to the fact that we do not know the time origin and carrier phase.

We can write the tap gain functions in terms of $x_s(t)$ and $x_c(t)$.

$$a_\nu(t) = \alpha_\nu[x_c(t)\cos(\Delta\omega t+\psi) - x_s(t)\sin(\Delta\omega t+\psi)] \tag{24}$$

$$b_\nu(t) = \alpha_\nu[x_c(t)\sin(\Delta\omega t+\psi) + x_s(t)\cos(\Delta\omega t+\psi)]. \tag{25}$$

If we make the assumption that $x_s(t)$ and $x_c(t)$ are (strict sense) stationary processes, we can determine what conditions they must satisfy in order for $a_\nu(t)$ and $b_\nu(t)$ to be stationary. Since for a stationary process the mean is independent of time, we see immediately that

$$E[x_c(t)] = E[x_s(t)] = 0 \tag{26}$$

is a necessary condition. As we show in Appendix B, we have further constraints. If, for instance, we assume x_s and x_c to be independent random variables, they must be Gaussian and have the same variance for $a_\nu(t)$ and $b_\nu(t)$ to be (strict sense) stationary. We have also conditions on the correlation functions for $x_s(t)$ and $x_c(t)$:

$$R_c(\tau) = R_s(\tau) \tag{27}$$

$$R_{sc}(\tau) = -R_{cs}(\tau) \tag{28}$$

is a necessary condition for $a_\nu(t)$ and $b_\nu(t)$ to be stationary.

If, in addition, $x_s(t)$ and $x_c(t)$ are sample functions from independent random processes, we obtain (see Appendix B) for the autocorrelation and crosscorrelation of a(t) and b(t)

$$R_a(\tau) = R_b(\tau) = R_c(\tau)\cos\Delta\omega\tau \tag{29}$$

$$R_{ba}(\tau) = -R_{ab}(\tau) = R_c(\tau)\sin\Delta\omega\tau \tag{30}$$

This means that as long as $\Delta\omega \neq 0$, a(t) and b(t) cannot be independent processes. The conclusions that we can draw are that even if the ionosphere is stationary, our tap gain functions are only stationary under rather restricted conditions. If instead of characterizing each pair of taps on the delay line with the functions $a_\nu(t)$ and $b_\nu(t)$ we consider the amplitude

$$V(t) = \sqrt{a_\nu^2(t) + b_\nu^2(t)} = \alpha_\nu A(t) \tag{31}$$

and phase

$$\theta(t) = \operatorname{arctg}\frac{b_\nu(t)}{a_\nu(t)} = \phi(t) + \Delta\omega t + \psi, \tag{32}$$

we are in a somewhat better position because V(t) is stationary even if $E[A(t)] \neq 0$.

$\theta(t)$ is still not stationary for it contains a term increasing linearly with time, but it should at least be easier to compensate for that effect than if we deal with $a_\nu(t)$ and $b_\nu(t)$.

Nevertheless, the delay-line model is still rather complicated. If we want to work in real time, we have to introduce a delay that can be inconvenient. The number of taps that are necessary for a particular purpose is hard to estimate; for the simple case of a single path with delay the magnitude of the taps decreases as $1/\nu$, where ν is the number of taps. Another thing is, that even if our channel consists of a number of statistically independent paths with different delays, the tap functions need not be uncorrelated. We saw in the case of a single path that all the tap functions had identical form and hence had correlation equal to one.

2.3 A PHYSICAL MODEL OF THE IONOSPHERE

Thus far, we have seen that it should be possible to represent ionospheric transmission by a tapped delay-line model. The complexity of such a representation, however, turned out to be rather high, even for simple multipath structures.

To avoid some of the difficulties, we shall use instead a model that takes into account what is known about the multipath structure of the ionosphere. We are, of course, losing something in generality but we gain in simplicity.

The model that we utilize is the same as the one used by Turin,[21] except that we allow a frequency shift caused by Doppler shift or offset of the local oscillator in the receiver.

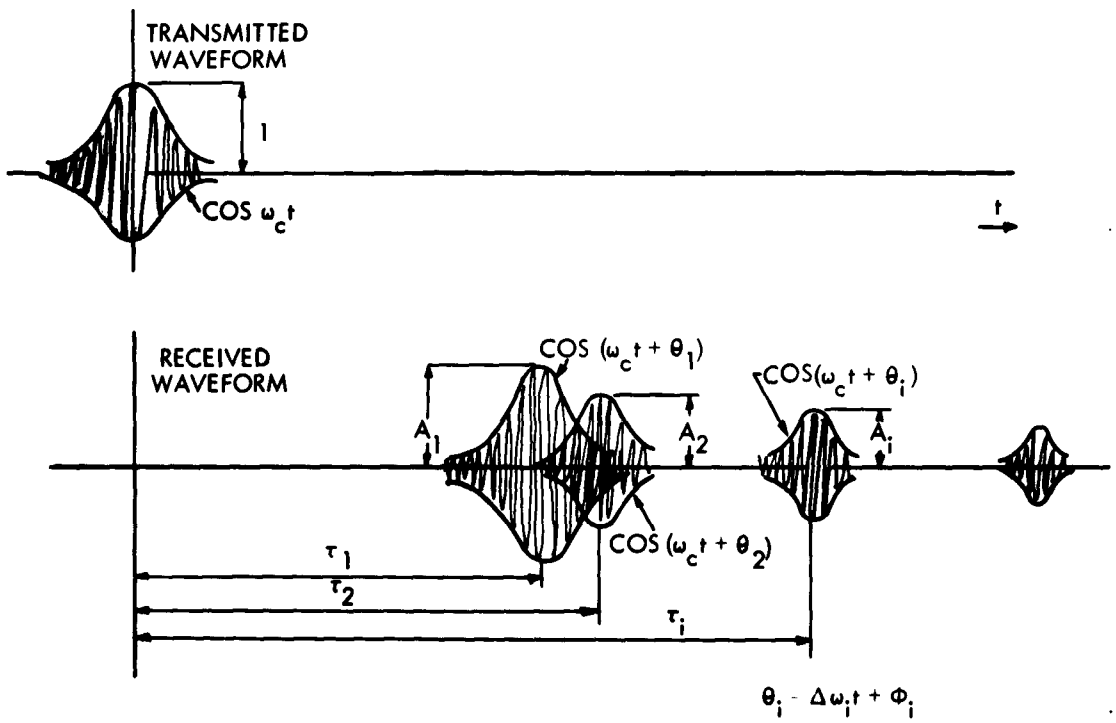

Fig. 14. Model of ionospheric scattering propagation.

We assume that it is possible, for our purposes, to represent the ionosphere by a number of paths, each of which has associated with it an amplitude A_i, a phase θ_i, and a delay τ_i. These qualities change slowly with time so that they can be considered as constants during the transmission of a signal. θ_i is of the form $\omega_i t + \phi_i(t)$, but for the time being we make no assumptions of stationariness of $A_i(t)$, $\tau_i(t)$ or $\phi_i(t)$. See Fig. 14.

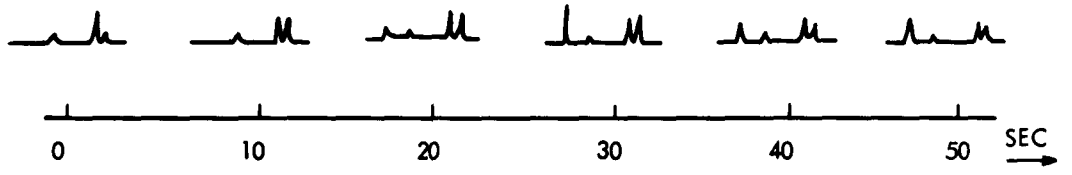

Fig. 15. Impulse responses of ionospheric scattering taken 10 seconds apart.

The validity of this model can, of course, only be proved by comparing it with physical data. The knowledge of HF ionospheric transmission that has been published is not too extensive, and the facts that support the model are, for the most part, of speculative character. In Fig. 15 there are some pictures of the received signal over a 1685-km ionospheric scattering link at 12.35 mc when a short pulse (35 μsec) was transmitted. We see that the paths are well defined and their relative delay seems to stay constant, at least for times of the order of minutes. The response functions are taken from a note by Balser, Smith, and Warren.[2]

III. METHODS OF PREDICTION

3.1 INTRODUCTION

According to our communication scheme the receiver measures the parameters of the channel model utilizing a sounding signal and then predicts the behavior of the channel for the time interval used for message transmission. The fluctuations in the ionosphere are random and, accordingly, the parameters in the model are determined by random processes. Thus, what we need is a prediction in a statistical sense, and we have the restriction that only a limited part of the past of the process is available. As we have pointed out, there is no evidence that the statistics of the ionosphere should be particularly simple, or even stationary. Our prediction operation should therefore not be sensitive to what kind of process it is applied to, and it is also desirable for it to be easily instrumented.

In the first part of this section some simple operations suitable for pure prediction are discussed and compared with optimum linear prediction. In the last part the problem of prediction in the presence of noise is considered and some calculations are carried out on ionospheric data.

3.2 PURE PREDICTION

a. Last-Value Prediction

Perhaps the simplest prediction operation, when the function is known only in the vicinity of a point, is to use the value at the point as a prediction. See Fig. 16. In the following discussion we use the term "last-value prediction" for that kind of operation. For a random process s(t) the error at prediction time T is

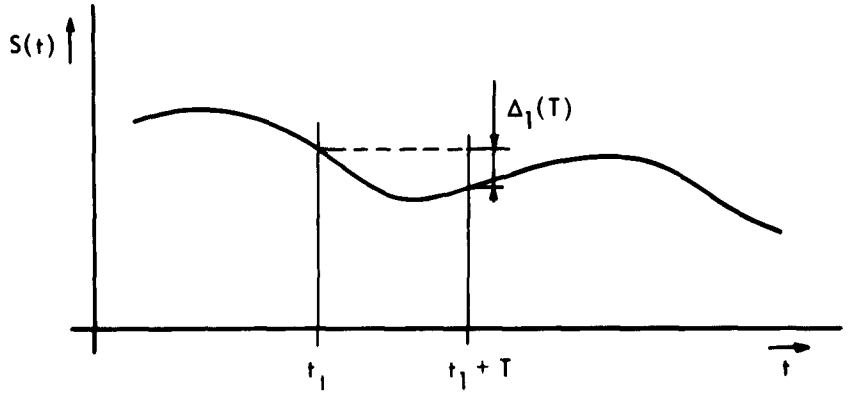

Fig. 16. Last-value prediction.

$$\Delta_1(T) = s(t_1+T) - s(t_1), \tag{33}$$

and the mean-square error is

$$E[\Delta_1^2(T)] = E[s^2(t_1+T) - 2s(t_1+T)\,s(t_1) + s^2(t_1)] = 2[R(0)-R(T)],$$

where R(T) is the autocorrelation function (with the mean subtracted out) of s(t). If we define the correlation time τ_c as

$$R(\tau_c) = \frac{1}{2} R(0), \tag{34}$$

we see that

$$E[\Delta_1^2(T)] > R(0) \qquad \text{for } T > \tau_c$$

which means that the method is not suitable for $T > \tau_c$, since we then get a greater mean-square error than the variance of the process itself. We notice that we do not use any statistical property of the process with this simple prediction.

b. Maximum Likelihood Prediction

If we know the second-order probability distribution for the process, we can use the value of $s(t_1+T)$ that maximizes $p(s(t_1+T)/s(t_1))$ as a prediction. We call this "maximum likelihood" prediction and investigate the case of Gaussian statistics, in which the second-order statistics are completely determined by the autocorrelation function.

For a zero-mean Gaussian process, $p(s(t_1+T)/s(t_1))$ is a Gaussian distribution with

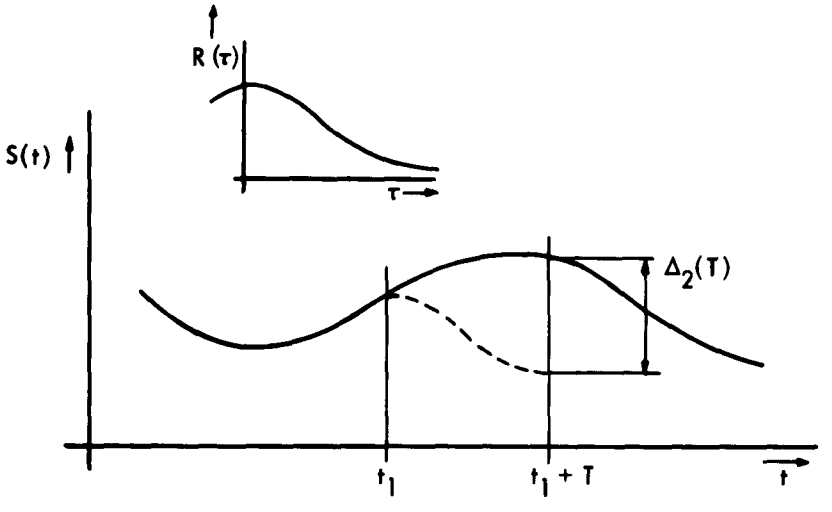

Fig. 17. Maximum likelihood prediction (Gaussian Case).

mean $\frac{R(T)\, s(t_1)}{R(0)}$ and variance $R(0)\left[1-\left(\frac{R(T)}{R(0)}\right)^2\right]$. Since the Gaussian distribution is maximum at the mean, this simply means we use the autocorrelation function as predictor (see Fig. 17). The mean-square error for prediction time T is

$$E[\Delta_2^2(T)] = E\left[\left(s(t_1+T) - \frac{R(T)\, s(t_1)}{R(0)}\right)^2\right] = R(0) - \frac{R^2(T)}{R(0)}. \tag{35}$$

We see that for small T the error is the same as for last-value prediction, but for large T maximum likelihood prediction is better because $E[\Delta_2^2(T)]$ can never exceed the variance of the process.

For $T = \tau_c$, $E[\Delta_2^2(\tau_c)] = 3/4\ R(0)$. We notice that for a first-order Markov process this kind of prediction is actually optimum. The reason for this is simply that the future behavior of the process is completely determined, in a statistical sense, by the last value.

c. Tangent Prediction

If we use the tangent of the curve as a predictor, we have another possible way of simple prediction, using only knowledge of the process around a single point.

Before we can discuss this type of prediction, we need to look into the question of derivatives of stochastic processes.

Derivatives of a Random Process

Consider a random process x(t) with variance σ_x and mean m_x. Define a function

$$y(t, \tau) = \frac{x(t+\tau) - x(t)}{\tau} \qquad \tau \neq 0. \tag{36}$$

We have

$$E[y(t, \tau)] = 0$$

$$E[y^2(t, \tau)] = \frac{1}{\tau^2} E[x^2(t+\tau) - 2x(t)\, x(t+\tau) + x^2(t)] = \frac{2}{\tau^2}[R(0) - R(\tau)].$$

When $\tau \to 0$, $y(t, \tau)$ is equal to $\frac{dx(t)}{dt}$, therefore the derivative has a finite variance only if $[R(0)-R(\tau)]$ goes to zero at least as fast as τ^2. Since $R(\tau)$ is an even function, either

$$R'(0) = 0 \quad \text{or} \quad R'(+0) = -R'(-0).$$

In the last case the second derivative at zero does not exist, and differentiability of a random process is equivalent to requiring that $R'(0)$ exists. We can state this in terms of the power density spectrum:

$$R''(0) = -4\pi^2 \int_{-\infty}^{\infty} f^2\, S(f)\, df. \tag{37}$$

A sufficient and necessary condition for the derivative of a random process to exist (with probability one) is

$$\int_{-\infty}^{\infty} f^2 S(f)\, df < \infty.$$

See Doob[25] for a rigorous proof.

In the following we assume that the derivative of the random process exists and we thus have

$$E[(x'(t))^2] = -R''(0) \tag{38}$$

Finally we remark, that since the derivative is a linear function of the original process, the derivative of a Gaussian process has a Gaussian distribution with zero mean and variance $R''(0)$.

As an example of processes which have no derivative, we can take the first order Markov process. It has an autocorrelation of the form

$$R(\tau) = R(0)\, e^{-\alpha|\tau|} \tag{39}$$

(see Doob[26] for a proof). This function has no second derivative at the origin and a sample function from the Markov process has no derivative (with probability one) at any point. This explains why the optimum linear predictor takes such a simple form as an exponential attenuator.

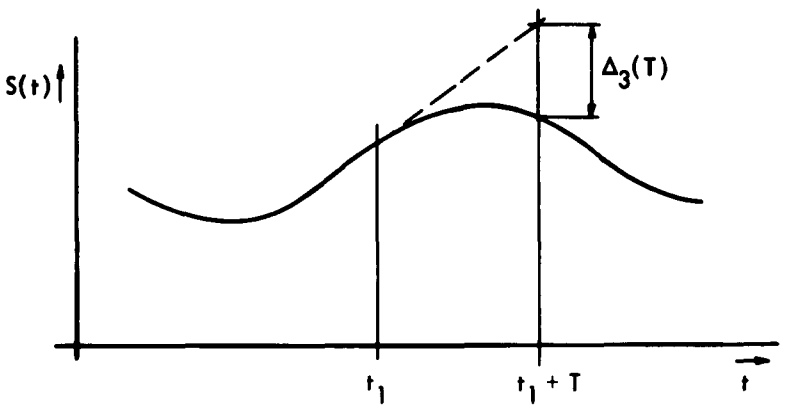

Fig. 18. Tangent prediction.

Tangent Prediction

We obtain the error for prediction time T (see Fig. 18)

$$\Delta_3(T) = s(t_1+T) - [s(t_1)+Ts'(t_1)]. \tag{40}$$

The mean-square error is

$$E[\Delta_3^2(T)] = E[s^2(t_1+T)+s^2(t_1)+T^2(s'(t_1))^2-2s(t_1+T)s(t_1)-2Ts(t_1+T)s'(t_1)+2Ts(t_1)s'(t_1)].$$

To evaluate this, we notice that

$$E[s(t_1)s'(t_1)] = \lim_{\tau\to 0} E\left[s(t_1)\frac{s(t_1+\tau) - s(t_1)}{\tau}\right] = \lim_{\tau\to 0}\frac{1}{\tau}[R(\tau)-R(0)]$$

$$= R'(0) = 0$$

according to our assumption of differentiability. In the same way,

$$E[s(t_1+T)s'(t_1)] = -R(T)$$

and we have

$$E[\Delta_3^2(T)] = 2[R(0)-R(T)-\frac{T^2}{2}R''(0)+TR'(T)] = \Gamma(T). \tag{41}$$

We call this the function for $\Gamma(T)$, and by comparing it with the error for last-value prediction we can write

$$\Gamma(T) = E[\Delta_3^2(T)] = E[\Delta_1^2(T)] - T[TR''(0)-2R'(T)]. \tag{42}$$

As can be seen from Eq. 36, $R''(0)$ is always negative; and for a monotonically decreasing autocorrelation $R'(T)$ is negative for all T. In this case tangent prediction is better than the last-value prediction, at least for small values of T.

To get some insight into the expected performance of the different simple prediction schemes and to be able to compare them with optimum linear prediction, we work out a few examples, assuming certain forms of the autocorrelation function.

d. Examples

Example 2

Let us first compare the simple prediction methods for the autocorrelation of the form

$$R(\tau) = R(0)\exp\left(-\frac{\tau^2}{\tau_0^2}\right). \tag{43}$$

In this case

$$E[\Delta_1^2(T)] = 2R(0)\left[1 - \exp\left(-\frac{T^2}{\tau_0^2}\right)\right] \tag{44}$$

$$E[\Delta_2^2(T)] = R(0)\left[1 - \exp\left(-\frac{2T^2}{\tau_o^2}\right)\right] \tag{45}$$

$$\Gamma(T) = R(0)\left[1 + \frac{T^2}{\tau_o^2} - \left(1 + 2\frac{T^2}{\tau_o^2}\right)\exp\left(-\frac{T^2}{\tau_o^2}\right)\right] \tag{46}$$

$$\tau_c = \tau_o\sqrt{\ln 2}$$

These functions are plotted in Fig. 19, and we see that as long as $T < \tau_c$ the tangent prediction gives the smallest error.

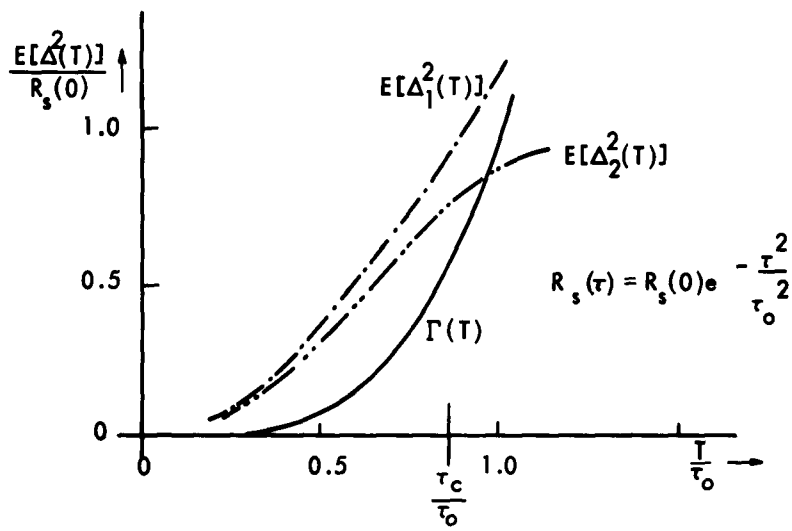

Fig. 19. Comparison between simple predictions (Example 2).

Example 3

To be able to compare with optimum linear prediction, consider a process with power density spectrum

$$S_2(f) = \frac{k^2}{(a^2+f^2)^2} . \tag{47}$$

The corresponding autocorrelation is the Fourier transform of S(f). Applying residue calculus, we have

$$R_2(\tau) = 2\pi j \operatorname{Res}\left[\frac{k^2 e^{j2\pi f\tau}}{(a^2+f^2)^2}\right]_{f=ja} \qquad (\tau > 0)$$

which gives

$$R_2(\tau) = \sigma_2^2 \left[1 + \frac{|\tau|}{\tau_o}\right] \exp\left(-\frac{|\tau|}{\tau_o}\right), \tag{48}$$

where $\sigma_2^2 = \frac{k^2\pi}{2a^3}$ and $\tau_o = \frac{1}{2\pi a}$. $R_2(\tau)$ is plotted in Fig. 20, from which we see that the correlation time τ_c is approximately $1.7\tau_o$.

To evaluate the error of the optimum predictor, we take the "realizable part" of $S_2(f)$.

$$G_2(f) = \frac{k}{(ja-f)^2}$$

and the corresponding function in the time domain is

$$g_2(t) = \int_{-\infty}^{\infty} \frac{k\, e^{j2\pi ft}}{(ja-f)^2}\, dt = 2\pi j \text{ Res} \left[\frac{k\, e^{j2\pi ft}}{(ja-f)^2}\right]_{f=ja} \qquad (t>0)$$

which gives

$$g_2(t) \begin{cases} = k4\pi^2 t\, e^{-\frac{t}{\tau_o}} & t \geq 0 \\ = 0 & t < 0. \end{cases} \tag{49}$$

The mean-square error for the optimum linear predictor for prediction time T is

$$\epsilon(T) = \int_0^T |g(t)|^2\, dt.$$

(See Davenport and Root[27] for a derivation.) In our particular case we have

$$\epsilon_2(T) = k^2 16\pi^4 \int_0^T t^2 \exp\left(-\frac{2t}{\tau_o}\right) dt = \sigma_2^2 \left[1 - \left(1 + 2\frac{T}{\tau_o} + 2\frac{T^2}{\tau_o^2}\right)\exp\left(-\frac{2T}{\tau_o}\right)\right]. \tag{50}$$

To get the error for the tangent predictor we obtain from Eq. 48

$$R_2''(0) = -\frac{\sigma_2^2}{\tau_o^2}$$

$$R_2'(T) = -\sigma_2^2 \frac{T}{\tau_o^2} e^{-\frac{T}{\tau_o}}$$

which by substitution in (41) yields

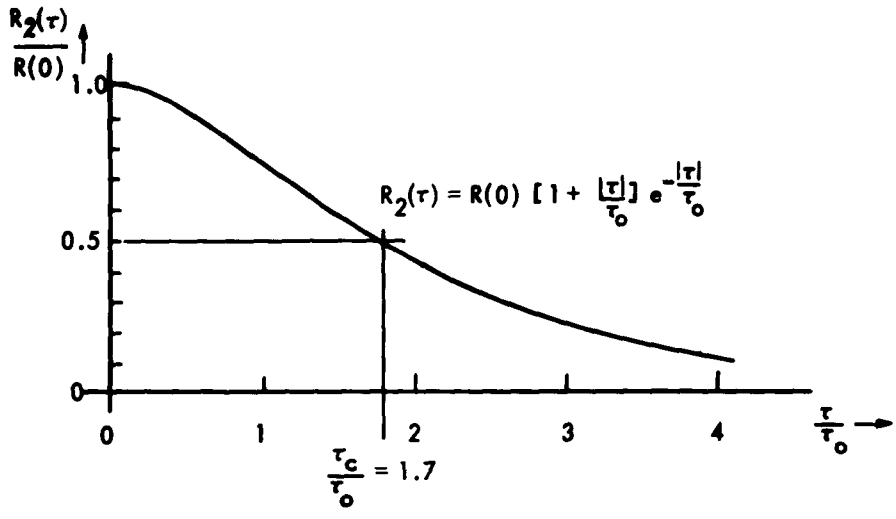

(a)

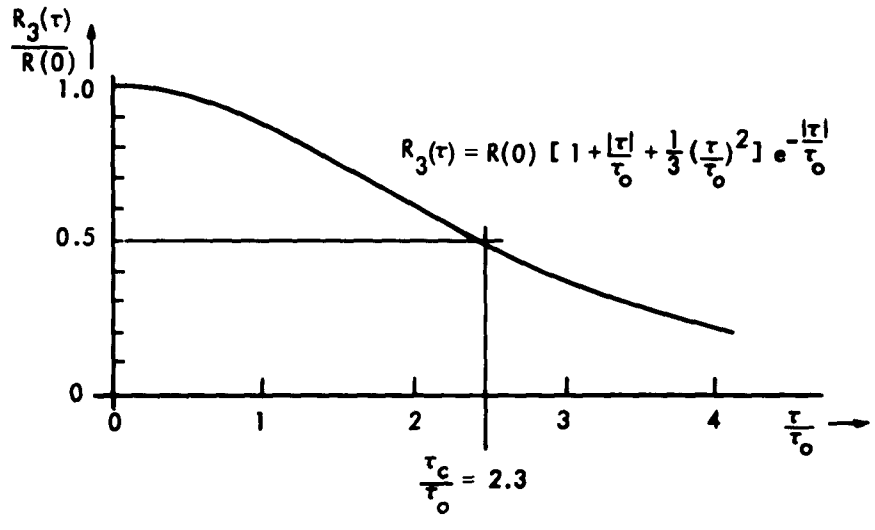

(b)

Fig. 20. Autocorrelation functions in Examples 3 and 4.

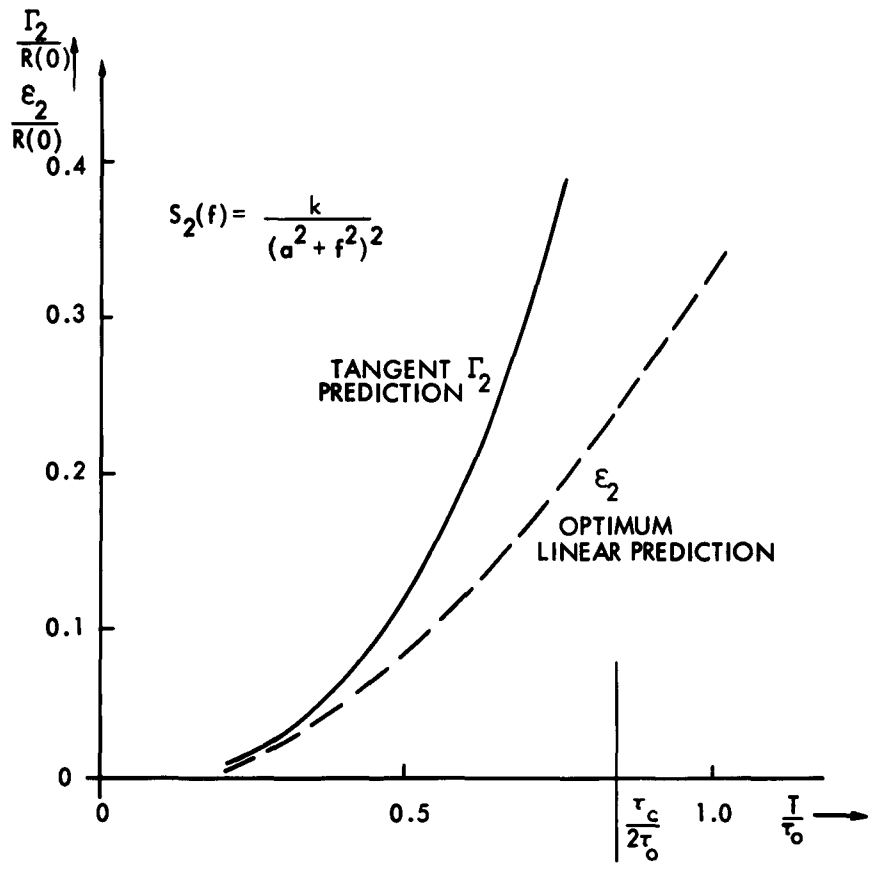

Fig. 21. Tangent prediction compared with optimum prediction (Example 3).

$$\Gamma_2(T) = 2\sigma_2^2 \left[1 + \frac{1}{2}\frac{T^2}{\tau_o^2} - \left(1 + \frac{T}{\tau_o} + \frac{T^2}{\tau_o^2}\right)\exp\left(-\frac{T}{\tau_o}\right)\right]. \tag{51}$$

In Fig. 21, $\epsilon_2(T)$ and $\Gamma_2(T)$ are plotted. We notice that when $T \ll \tau_o$

$$\epsilon_2(T) \approx \Gamma_2(T) \approx \frac{4}{3}\sigma_2^2 \left(\frac{T}{\tau_o}\right)^3.$$

The tangent prediction is thus "asymptotically optimum" in this special case. The reason is rather obvious. Since the fourth derivative of $R_2(\tau)$ does not exist at zero, the sample functions do not have a second derivative and it is not surprising that the optimum prediction is essentially linear extrapolation for small prediction time.

A more complete discussion of optimum prediction for this particular correlation function has been given by Lee.[13]

Example 4

Consider a random process in which the sample functions have derivatives of higher order than the first.

Take

$$S_3(f) = \frac{k^2}{(a^2+f^2)^3} \tag{52}$$

In this case we have

$$R_3(\tau) = \sigma_3^2 \left[1 + \frac{|\tau|}{\tau_o} + \frac{1}{3}\frac{\tau^2}{\tau_o}\right] e^{-\frac{|\tau|}{\tau_o}}, \tag{53}$$

where

$$\sigma_3^2 = \frac{k^2 3\pi}{8a^5} \quad \text{and} \quad \tau_o = \frac{1}{2\pi a}.$$

$R_3(\tau)$ is plotted in Fig. 20 which gives a correlation time τ_c of approximately $2.3\tau_o$.

$$G_3(f) = \frac{k}{(ja-f)^3}$$

$$g_3(t) \begin{cases} = k4\pi^3 t^2 e^{-\frac{t}{\tau_o}} & t \geq 0 \\ = 0 & t < 0 \end{cases} \tag{54}$$

which gives the mean-square errors

$$\epsilon_3(T) = \sigma_3^2 \left[1 - \left(1 + 2\frac{T}{\tau_o} + 2\frac{T^2}{\tau_o^2} + \frac{4}{3}\frac{T^3}{\tau_o^3} + \frac{2}{3}\frac{T^4}{\tau_o^4}\right) e^{-\frac{2T}{\tau_o}}\right] \tag{55}$$

$$\Gamma_3(T) = 2\sigma_3^2 \left[1 + \frac{1}{6}\frac{T^2}{\tau_o^2} - \left(1 + \frac{T}{\tau_o} + \frac{2}{3}\frac{T^2}{\tau_o^2} + \frac{1}{3}\frac{T^3}{\tau_o^3}\right) e^{-\frac{T}{\tau_o}}\right]. \tag{56}$$

In Fig. 22, $\epsilon_3(T)$ and $\Gamma_3(T)$ are plotted. For small values of T we have

$$\epsilon_3(T) \approx \frac{4}{15}\sigma_3^2 \left(\frac{T}{\tau_o}\right)^5$$

$$T \ll \tau_o$$

$$\Gamma_3(T) \approx \frac{1}{4}\sigma_3^2 \left(\frac{T}{\tau_o}\right)^4$$

In this case the tangent prediction gives a one order of magnitude larger error for small prediction time. According to Fig. 22 it is nevertheless performing rather well compared with optimum prediction as long as the prediction time is shorter than the

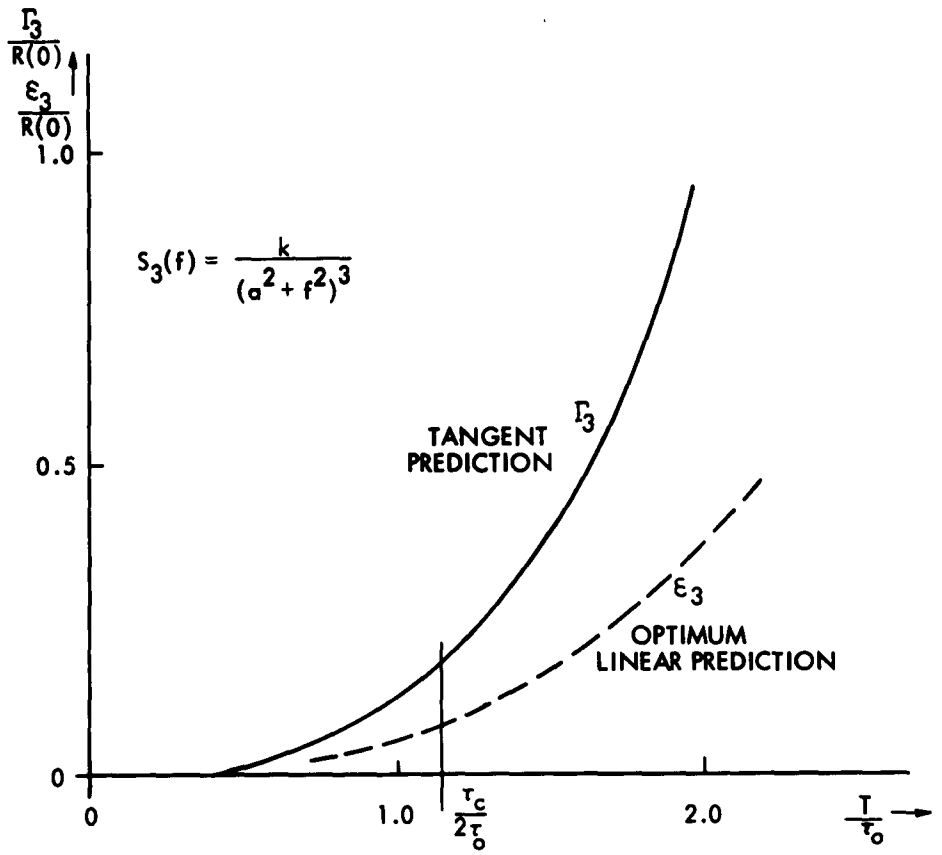

Fig. 22. Tangent prediction compared with optimum prediction (Example 4).

correlation time.

As long as we are working with power density spectra that are rational functions, the integral

$$\int_{-\infty}^{\infty} f^{2n} S(f)\, df$$

is not convergent for n larger than a certain value, and accordingly the sample functions cannot have derivatives of arbitrarily high order. The two examples that we have given seem to indicate that it should be possible to obtain a prediction that is "asymptotically optimum" (for T approaching zero) by using the existing terms in the Taylor series expansion of the sample function. If we apply this point of view, tangent prediction can be considered as the first-order approximation of such an "asymptotically optimum" predictor.

e. Conclusions

It is difficult to make any general statements on the basis of a few examples, but the previous discussion supports the view that tangent prediction should not be an

unreasonable thing to do, at least under certain circumstances. To be able to construct an optimum predictor, we need to know the power density spectrum, or autocorrelation function, of the process. The tangent prediction, on the other hand, does not use any statistical properties of the process and it is simple to instrument. Since obtaining the derivative is a linear process, tangent prediction is, of course, always inferior to optimum linear prediction. If, on the contrary, we do not know the autocorrelation function accurately enough, or use a predictor design for a particular prediction time under a maximum time interval, we could perhaps do just as well with the simpler tangent prediction. The mean-square error of the optimum predictor can never exceed the variance of the process, but there is no limitation for the error of tangent prediction for large prediction time. If we want to employ tangent prediction, we must be sure that the prediction time is at least not greater than (say) the correlation time for the process. Moreover, we have seen that it is mainly useful only for random processes with monotonically decreasing autocorrelation functions.

We shall now modify the prediction operation in order to work with processes that are disturbed by noise.

3.3 SMOOTHING AND PREDICTION

Noise is often present together with the random process that is to be predicted. Tangent prediction cannot be expected to perform well in that case. Assume that we have a signal s(t), together with noise n(t), so that the wave that we have to work on to predict s(t) is y(t) = s(t) + n(t). The derivative of y(t) is s'(t) + n'(t), and, even if n(t) is much smaller than s(t), its derivative n'(t) need not be small compared with s'(t).

To employ the idea of tangent prediction and to be able to introduce the necessary smoothing operation, we assume that the random process y(t) is sampled at times δ seconds apart. If we use a certain number of samples to compute a regression line for use as a predictor, we have an operation that averages out the effects of the noise. In

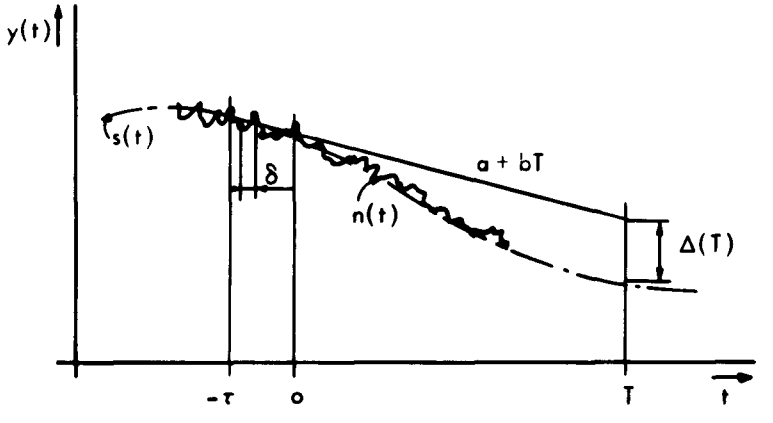

Fig. 23. Regression line prediction.

the noiseless case it is identical to tangent prediction when δ becomes very small. See Fig. 23.

a. Regression-Line Prediction

Let us state the problem more precisely and derive an expression for the mean-square error. Assume that we have samples of a wide sense stationary random process $y(t) = s(t) + n(t)$ sampled at times δ seconds apart. To predict $s(t)$ we use a straight line $a + bt$, where a and b are chosen so that

$$\Psi(a, b) = \sum_{\nu=0}^{N} [y(-\nu\delta)-(a-b\nu\delta)]^2 \tag{57}$$

is minimum. The expressions for a and b for the particular time origin chosen in Fig. 23 are given in Appendix C.

The mean-square error at prediction time T is

$$\Lambda(T) = E[(s(T)-(a+bT))^2]. \tag{58}$$

This expression is evaluated in Appendix C with the following assumptions: the noise has zero mean and is uncorrelated with the signal and is also uncorrelated between different samples. It is assumed that the time τ used to compute the regression line is short compared with the correlation time for the signal.

Under these assumptions, we have

$$\Lambda(T) = \Gamma(T) + \Psi(T)\left[\frac{\tau}{T} + \frac{N-1}{6N}\frac{\tau^2}{T^2}\right] + \frac{4}{N}\Phi(N)\sigma_n^2\left[3\frac{T^2}{\tau^2} + 3\frac{T}{\tau} + \frac{2N+1}{2N}\right]. \tag{59}$$

Here, $\Gamma(T)$ is the error for tangent prediction.

$$\Psi(T) = T^2(R_s''(T)-R_s''(0))$$

$$\Phi(N) = \frac{N^2}{(N+1)(N+2)}$$

$$\tau = N\delta$$

and $\sigma_n^2 = E[n^2(t)]$ is the variance of the noise.

Since we have the relation

$$R_s''(T) = -4\pi^2\int_{-\infty}^{\infty} f^2 S_s(f)\, e^{j2\pi fT}\, df \geq -4\pi^2\int_{-\infty}^{\infty} f^2 S_s(f)\, df = R_s''(0),$$

we see that $\Psi(T) \geq 0$, and regression-line prediction thus always gives a greater error than tangent prediction.

The second term in $\Lambda(T)$ is increasing for increasing τ and it is possible to interpret it as being due to the fact that the regression time is equal to the derivative only

when τ goes to zero. The third term depends on the noise. Since we have assumed that the noise is uncorrelated between samples, it is natural to get the result that the term decreases as 1/N for large N. This means that it is advantageous to increase the sampling rate, at least as long as the noise is still uncorrelated between samples. Contrary to other smoothing operations, any attempt to filter out the noise before regression-line prediction only gives greater error.

b. Minimization of the Mean-Square Error

The second term in $\Lambda(T)$ is increasing and the third term is decreasing with τ, and for a given T and δ it is possible to minimize $\Lambda(T)$ by choosing τ properly.

Let us work this out for $N \gg 1$. We can write

$$\Lambda(T) \cong \Gamma(T) + \Psi(T)\left[\frac{T}{\tau} + \frac{1}{6}\frac{T^2}{\tau^2}\right] + \frac{4\delta\sigma_n^2}{\tau}\left[3\frac{T^2}{\tau^2} + 3\frac{T}{\tau} + 1\right].$$

If we call $\tau/T = a$, we get

$$\frac{\partial\Lambda(T)}{\partial\tau} = \frac{\Psi(T)}{T}\left[1+\frac{1}{3}a\right] - \frac{4\delta\sigma_n^2}{T^2}\left[\frac{9}{a^4} + \frac{6}{a^3} + \frac{2}{a^2}\right] = 0$$

$$\frac{4\sigma_n^2\delta}{\Psi(T)\,T} = \frac{a^4\left[\frac{1}{3}a+1\right]}{2a^2 + 6a + 9} = \Omega_1(a). \tag{60}$$

The function $\Omega_1(a)$ is plotted in Fig. 24.

As an example, consider

$$R_s(t) = \sigma_s^2 \exp\left(-\frac{t^2}{\tau_o^2}\right)$$

with $\tau_o = 20$ sec; $T = 10$ sec; $\delta = 0.5 \times 10^{-3}$ sec (corresponding to $w_n = 10^3$ cps); and $\left(\frac{\sigma_n}{\sigma_s}\right)^2 = 10^{-3}$. We obtain $\Omega_1(a) = 6.7 \times 10^{-7}$. According to Fig. 24 the corresponding a is approximately 0.03 which gives $N = \frac{0.03 \times 10}{0.5 \times 10^{-3}} = 600$ and our assumption of N large is satisfied.

If we are not willing to compute the regression line by using more than a certain number of samples, we have another minimization problem. Given T and N, determine the δ that minimizes $\Lambda(T)$. Remembering that $a = \frac{\tau}{T} = \frac{N\delta}{T}$, we have

$$\frac{\partial\Lambda(T)}{\partial\delta} = \frac{\Psi(T)}{T}N\left[1 + \frac{N-1}{3N}a\right] - \frac{4\Phi(N)\sigma_n^2}{T}\left[6\frac{1}{a^3} + 3\frac{1}{a^2}\right] = 0$$

which gives

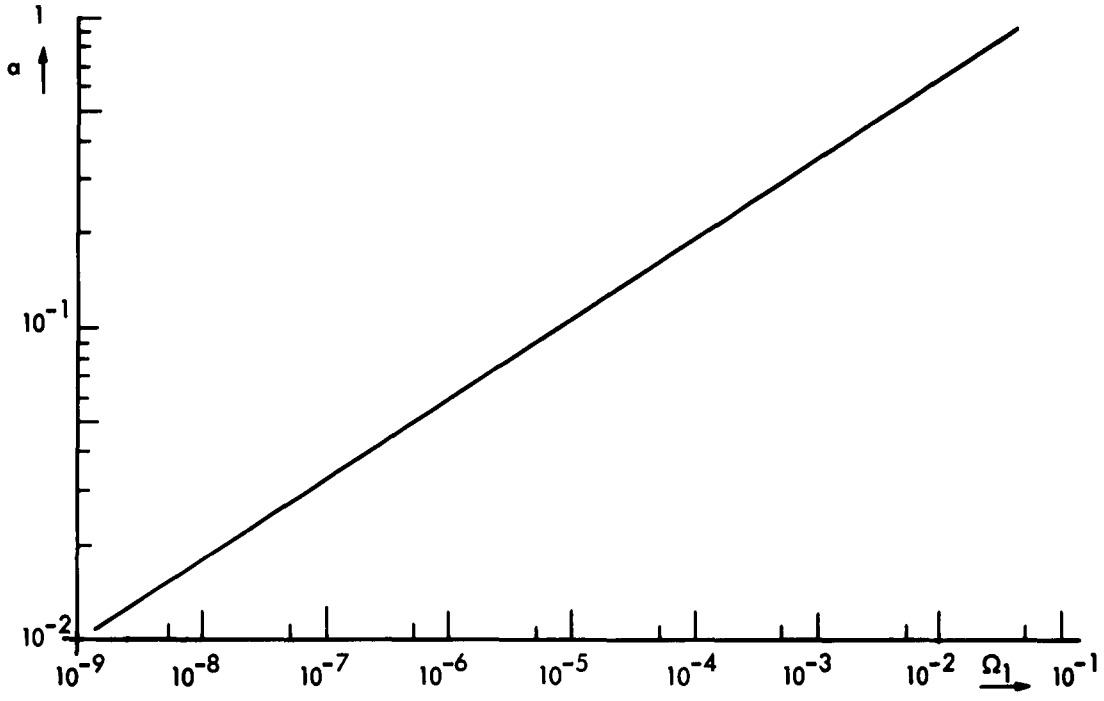

Fig. 24. The function $\Omega_1(a)$.

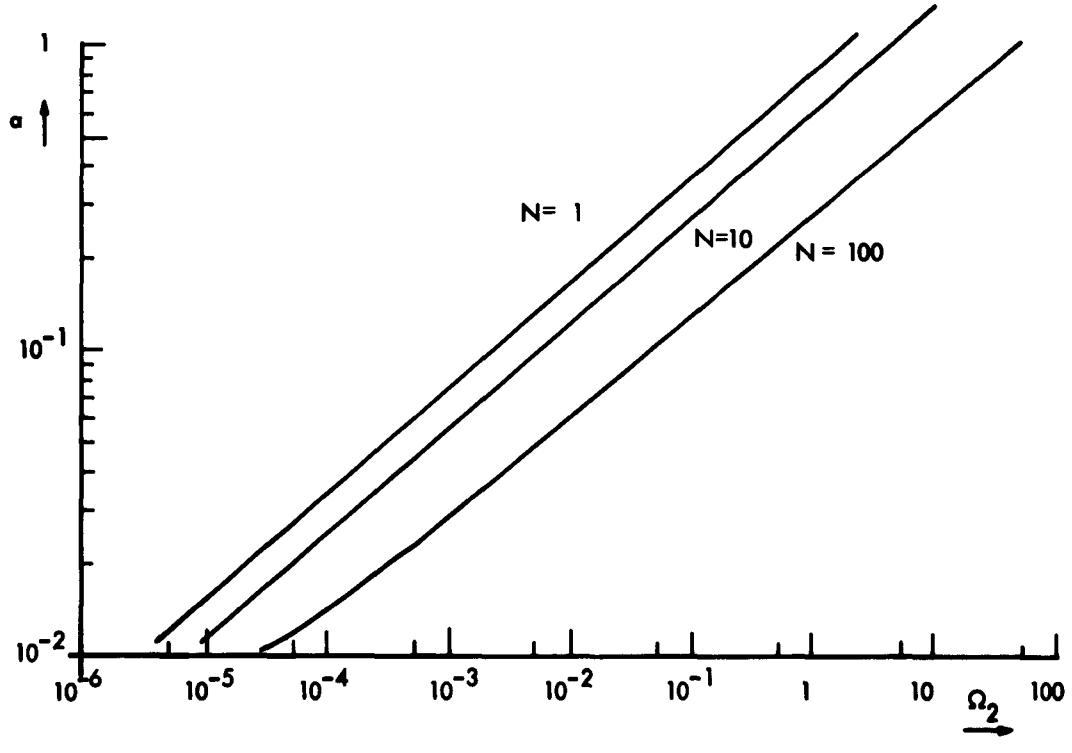

Fig. 25. The function (N, a).

$$\frac{12\sigma_n^2}{\Psi(T)} = \frac{Na^3\left[1+\frac{N-1}{3N}a\right]}{\Phi(N)[2+a]} = \Omega_2(N, a). \tag{61}$$

Ω_2 is plotted in Fig. 25 as a function of a for different values of N.

For the same example as before we get $\Omega_2(N, a) = 0.04$, which for N = 10 gives $a = 0.15$.

The practical value of these minimization procedures is limited by the fact that the derivation of $\Lambda(T)$ was made with the assumption of τ small.

3.4 COMPUTATIONS ON IONOSPHERIC DATA

a. Source of Data

The data were obtained from Group 34 of Lincoln Laboratory, M. I. T. The transmission link used was 1566 km from Atlanta, Georgia, to Ipswich, Massachusetts. A pulse of approximately Gaussian shape and bandwidth 30 kcps was transmitted every 1/15 sec with a transmitter peak power of 10 kw. Through a gating circuit at the receiver the maximum amplitude of the received pulses corresponding to the different paths was recorded. A "Datrac" equipment was used to quantize the samples into 64 levels and they were put onto magnetic tape as 6-bit numbers in a format corresponding to that for the IBM 709 computer. The records thus correspond to 6-bit samples of the path strength sampled 15 times a second.

b. Presentation of the Data

From a large collection of data two records were chosen rather arbitrarily. These were obtained on February 16, 1960, at 10:52 a. m. and 12:12 p. m. EST, respectively, and the carrier frequencies used were 8.35 mc and 18.45 mc, respectively. Of the first record, which we call A, 9724 samples were available corresponding to a recording time of approximately 11 minutes. Record A is probably a return from the F-layer of the ionosphere making 3 hops. In Fig. 26 it is plotted from the magnetic tape by the use of the computer. In the figure is also the identification word on the tape. The second recording, which we call B, contained 5271 samples, corresponding to approximately 6 minutes recording time. Record B is classified as a 1-hop F-layer return and it is plotted in Fig. 27.

Record A looks more stationary than record B and to show this the mean and variance, computed by using the first and second half of the record, are given below.

	Record A			Record B		
Part of record:	1st half	2nd half	Whole Record	1st half	2nd half	Whole Record
Mean	18.32	21.47	19.89	31.11	39.99	35.55
Variance	79.0	107.3	95.6	146.1	263.5	224.5

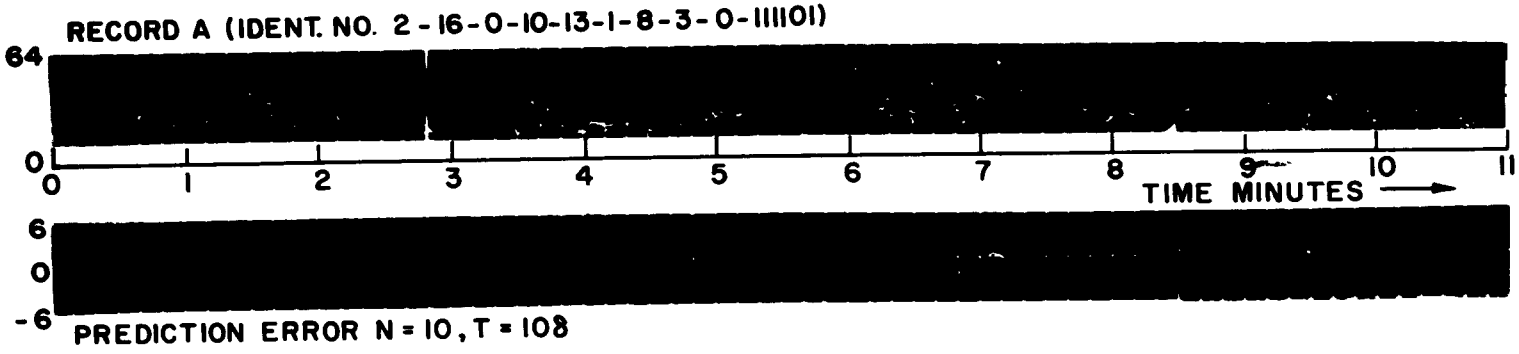

Fig. 26. Record A with prediction error.

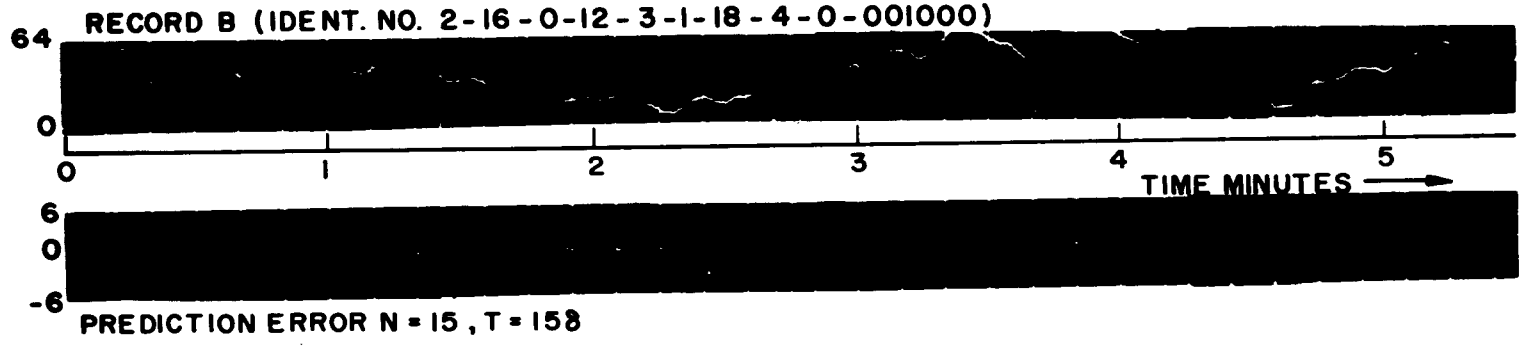

Fig. 27. Record B with prediction error.

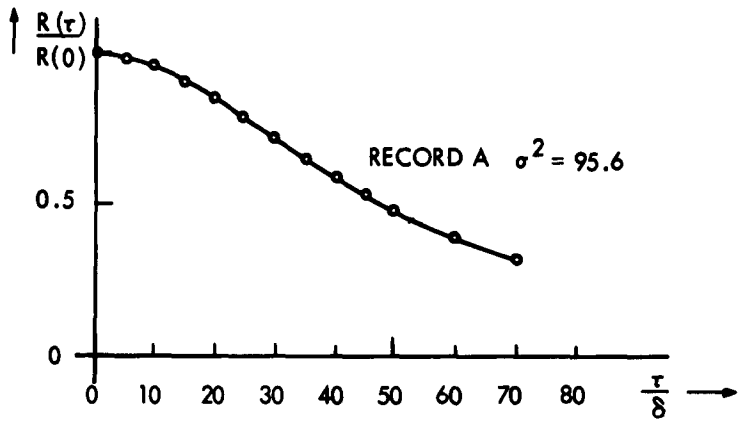

Fig. 28. Autocorrelation function, Record A.

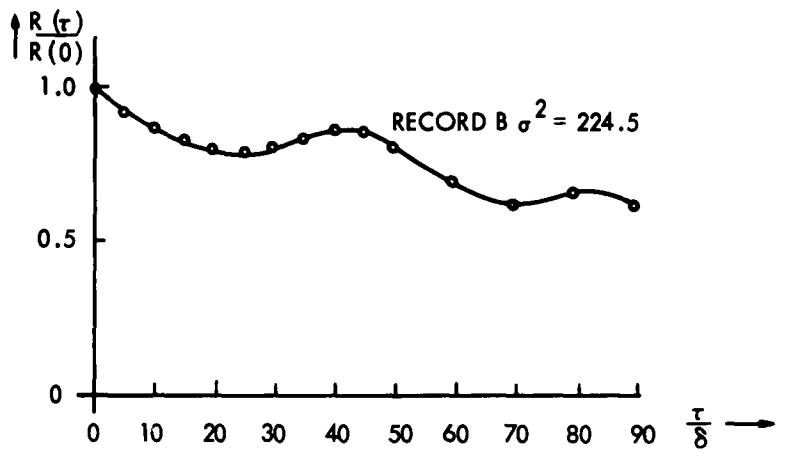

Fig. 29. Autocorrelation function, Record B.

Examination of the distribution functions for the records shows that Record A is approximately Rayleigh distributed; Record B is neither Rayleigh nor Rician.

The normalized autocorrelation functions for the records are presented in Figs. 28 and 29.

c. Results

Regression-line prediction was performed on the two records with the use of a computer. The computer calculated a regression line, using a certain number of samples corresponding to the prediction time T, and determined a new regression line. The prediction error was defined as the difference between the end of the old regression line and the beginning of the new one. The procedure was repeated through the whole record. In Figs. 30 and 31 the variance of the prediction error is plotted versus prediction time.

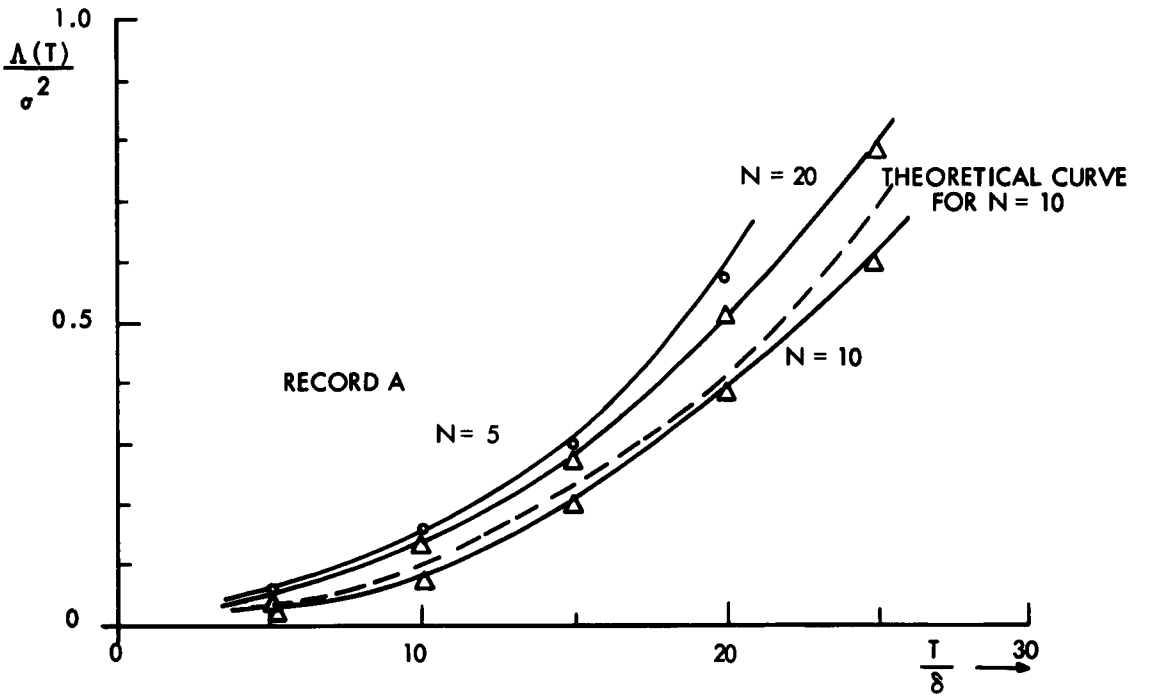

Fig. 30. Mean-square prediction error, Record A.

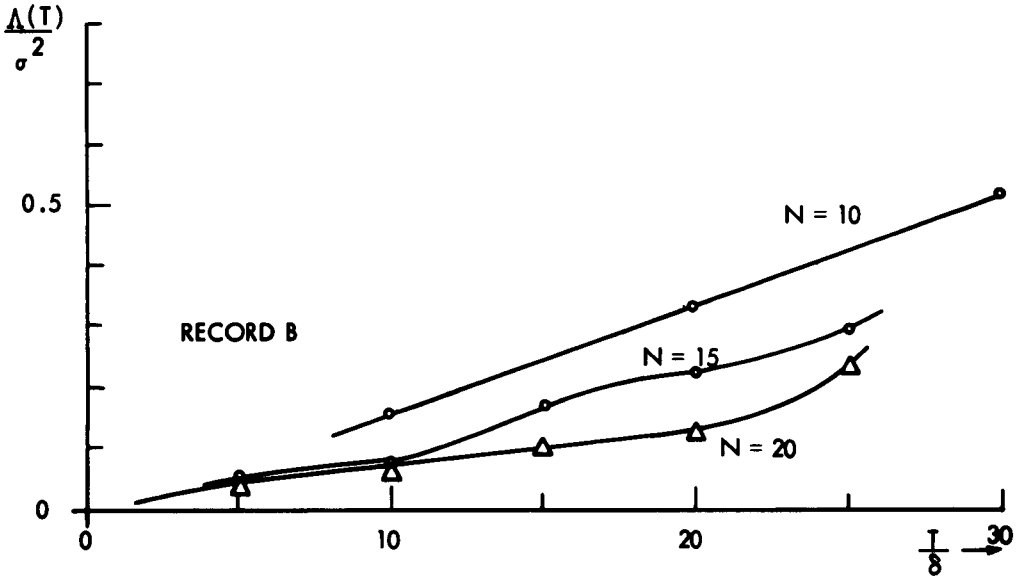

Fig. 31. Mean-square prediction error, Record B.

Different curves are given corresponding to number of samples used to compute the regression line. The statistics of the error were also computed and in Figs. 32 and 33 the distribution functions are given for different prediction times, plotted on normal distribution paper.

Record B is hardly stationary over the recording time. We can expect the prediction error to be more stationary than the process itself; and to illustrate this the prediction error is plotted below the corresponding record in Figs. 26 and 27.

To compare the calculated mean-square error with the theoretical formula (59) we need to know certain derivatives of the autocorrelation function and the signal-to-noise

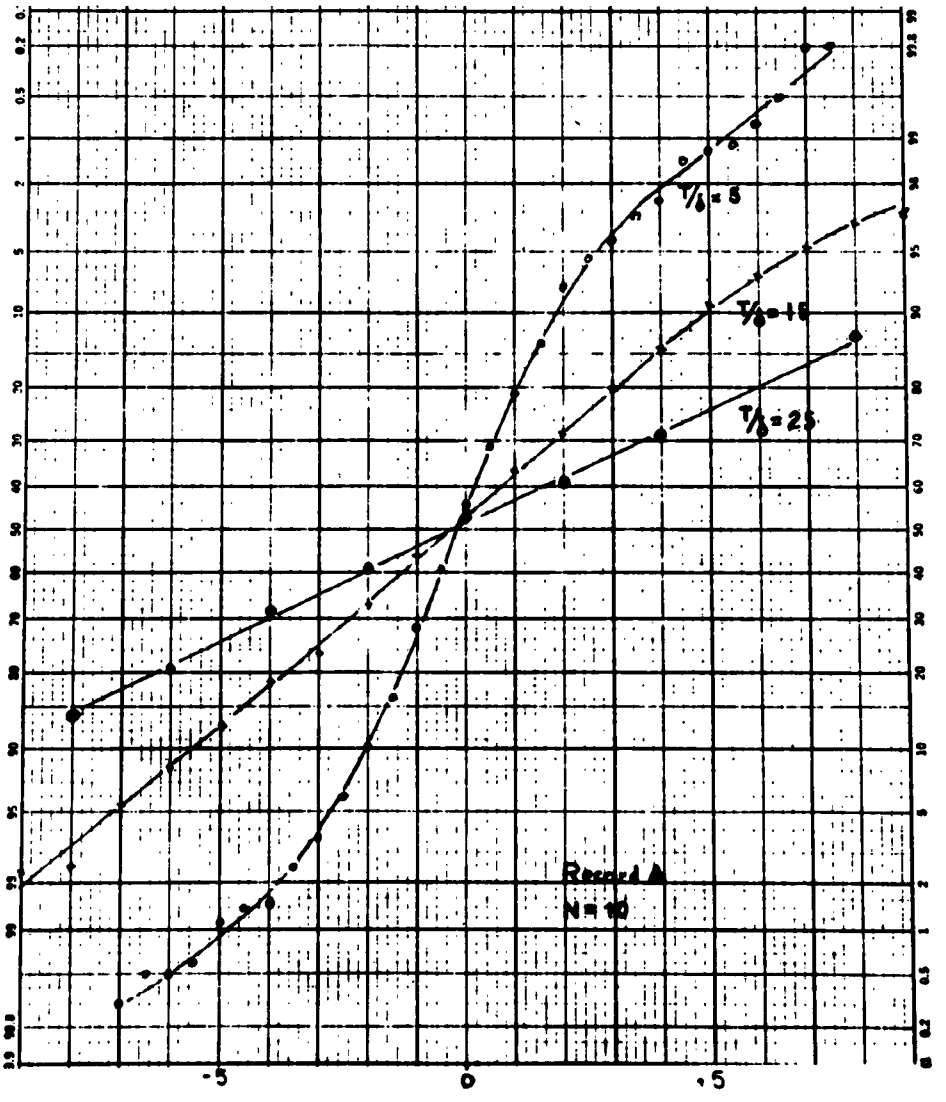

Fig. 32. Distribution functions for the error, Record A.

ratio for the record. The autocorrelation function used in Example 3 was used to represent that of Record A by making the correlation line τ_c for both curves to coincide. The signal-to-noise ratio for Record A was estimated to be 20 db, and the theoretical curve in Fig. 30 was obtained.

d. Discussion

The calculations performed show good correspondence with the theoretical results. It is interesting to notice that the correlation time for Record B is much longer than that for Record A, but Record B actually gives a larger prediction error. The reason is obvious if we compare the autocorrelation curves. When using regression-line prediction it is the behavior of the autocorrelation function around the origin that is of importance,

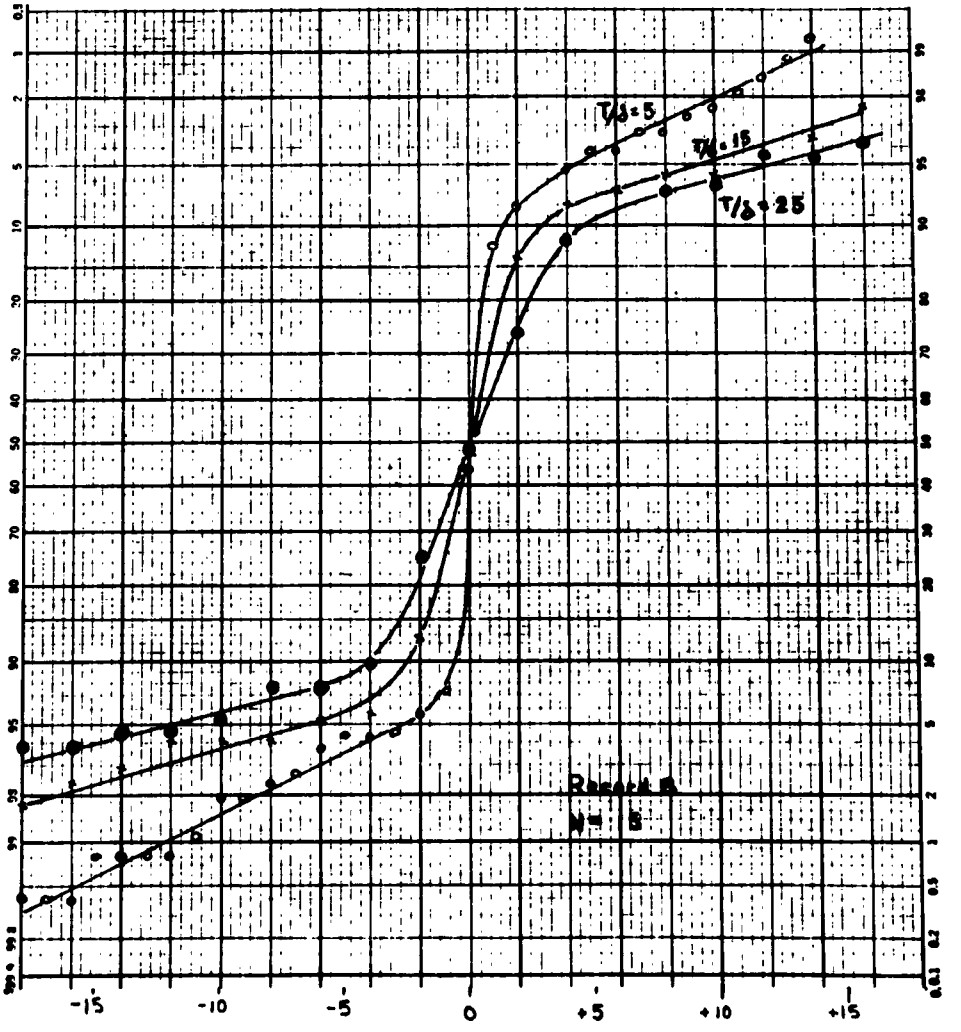

Fig. 33. Distribution functions for the error, Record B.

and we see that Record B actually has lower correlation for small correlation times than Record A.

According to Eq. 59, it is advantageous to use as many samples as possible to compute the regression line, as long as the noise is still independent between samples. From this point of view, the data are not sampled densely enough and it should be possible to reduce the time required to compute the regression line considerably.

Regression-line prediction should be useful in other applications as well. The effect of a slowly time-variant mean is suppressed in the prediction error, and regression-line prediction thus provides a way of dealing with certain types of nonstationary processes. In some applications it should be possible to characterize a fading medium by the prediction error and thereby greatly reduce the amount of data necessary for a description. The drop-outs in Record B give a number of large prediction errors and it is hard to say whether or not the distributions presented in Figs. 32 and 33 can be called approximately Gaussian. However, the statistics for the error in the two records seem to be more nearly alike than do the statistics for the two processes themselves.

IV. THE RECEIVER

4.1 INTRODUCTION

We have been dealing with the problem of choosing a useful model of scattering propagation and a method for measuring and predicting the parameters of the model. We arrived at a multipath model with slowly varying paths, each of which is characterized by an amplitude strength and a phase shift. By utilizing the prediction procedure presented in Section III, we can get an estimate of these quantities during the communication intervals. We assume that the Doppler shift (or frequency offset between transmitter and receiver) is small enough so that it is possible to make a reasonable prediction of the phase, and furthermore that the path delay can be considered constant between successive measurements of the channel.

The situation with which we are dealing is one in which the receiver has some knowledge about the random channel and we want to determine the best way to use this knowledge. To simplify the receiver, we assume that the decision is made on each received waveform separately and that we have no overlap between waveforms so that the received waveform, on which the decision is based, is due to only one transmitted waveform. This means that our receiver is not strictly optimum. The estimates of the channel parameters are certainly dependent within the prediction interval but probably not between intervals, and we hope that we are not too far off from optimum performance.

4.2 COMPLEX WAVEFORMS

To derive the receiver structure we use complex notation for bandpass functions. We shall now give a brief introduction to the needed concepts.

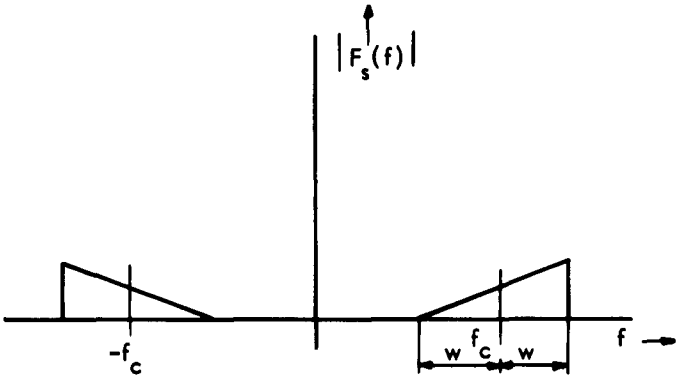

Fig. 34. Fourier transform of narrow-band real functions.

Assume that we have a real narrow-band function s(t) whose frequency spectrum (i.e., Fourier transform) is centered around the carrier frequency f_o. See Fig. 34. It is then possible to represent s(t) by a complex waveform $\xi(t)$, so that

$$s(t) = \mathrm{Re}\,[\xi(t)].$$

If we write

$$\xi(t) = x(t)\, e^{j\omega_o t},$$

we get

$$s(t) = \mathrm{Re}\,[x(t)]\cos\omega_o t - \mathrm{Im}\,[x(t)]\sin\omega_o t = x_c(t)\cos\omega_o t - x_s(t)\sin\omega_o t.$$

Here, $x_c(t)$ and $x_s(t)$ are the quadrature components of $s(t)$, and it is possible to show that

$$x_c(t) = \mathrm{Re}\left[2\int_0^\infty F_s(f)\, e^{j2\pi(f-f_o)t}\, df\right] \tag{62}$$

$$x_s(t) = \mathrm{Im}\left[2\int_0^\infty F_s(f)\, e^{j2\pi(f-f_o)t}\, df\right], \tag{63}$$

where $F_s(f)$ is the Fourier transform of $s(t)$. This shows that if $s(t)$ has bandwidth $2W$ around f_o, $x_c(t)$ and $x_s(t)$ are lowpass functions with bandwidth W.

It is also possible to represent the "complex amplitude" $x(t)$ by an amplitude and a phase angle

$$A_x(t) = |x(t)|, \quad \phi_x(t) = \angle\, x(t).$$

The complex notation is actually valid for an arbitrary $s(t)$, but it is especially useful for narrow-band functions, since $A_x(t)$ and $\phi_n(t)$ then correspond to the physical amplitude and phase of the signal.

We shall use correlation integrals involving complex waveforms, and it can be shown that for narrow-band signals

$$\mathrm{Re}\left[\int_0^T \xi^*(t)\,\eta(t)\,dt\right] = \int_0^T (x_c(t)\,y_c(t)+x_s(t)\,y_s(t))\,dt \cong 2\int_0^T s(t)\,n(t)\,dt \tag{64}$$

$$\mathrm{Im}\left[\int_0^T \xi^*(t)\,\eta(t)\,dt\right] = \int_0^T (x_c(t)\,y_s(t)-x_s(t)\,y_c(t))\,dt \cong 2\int_0^T s(t)\,\hat{n}(t)\,dt \tag{65}$$

$$\left|\int_0^T \xi^*(t)\,\eta(t)\,dt\right| = 2 \cdot \text{envelope of} \int_0^T s(t)\,n(t)\,dt, \tag{66}$$

where

$$s(t) = \mathrm{Re}\,[\xi(t)] = \mathrm{Re}\left[x(t)\, e^{j\omega_o t}\right]$$

$$n(t) = \mathrm{Re}\,[\eta(t)] = \mathrm{Re}\left[y(t)\, e^{j\omega_o t}\right].$$

($\hat{n}(t)$ denotes the Hilbert transform of $n(t)$. $n(t) = \hat{n}\left(t \frac{1}{4f_c}\right)$ for narrow-band function.)

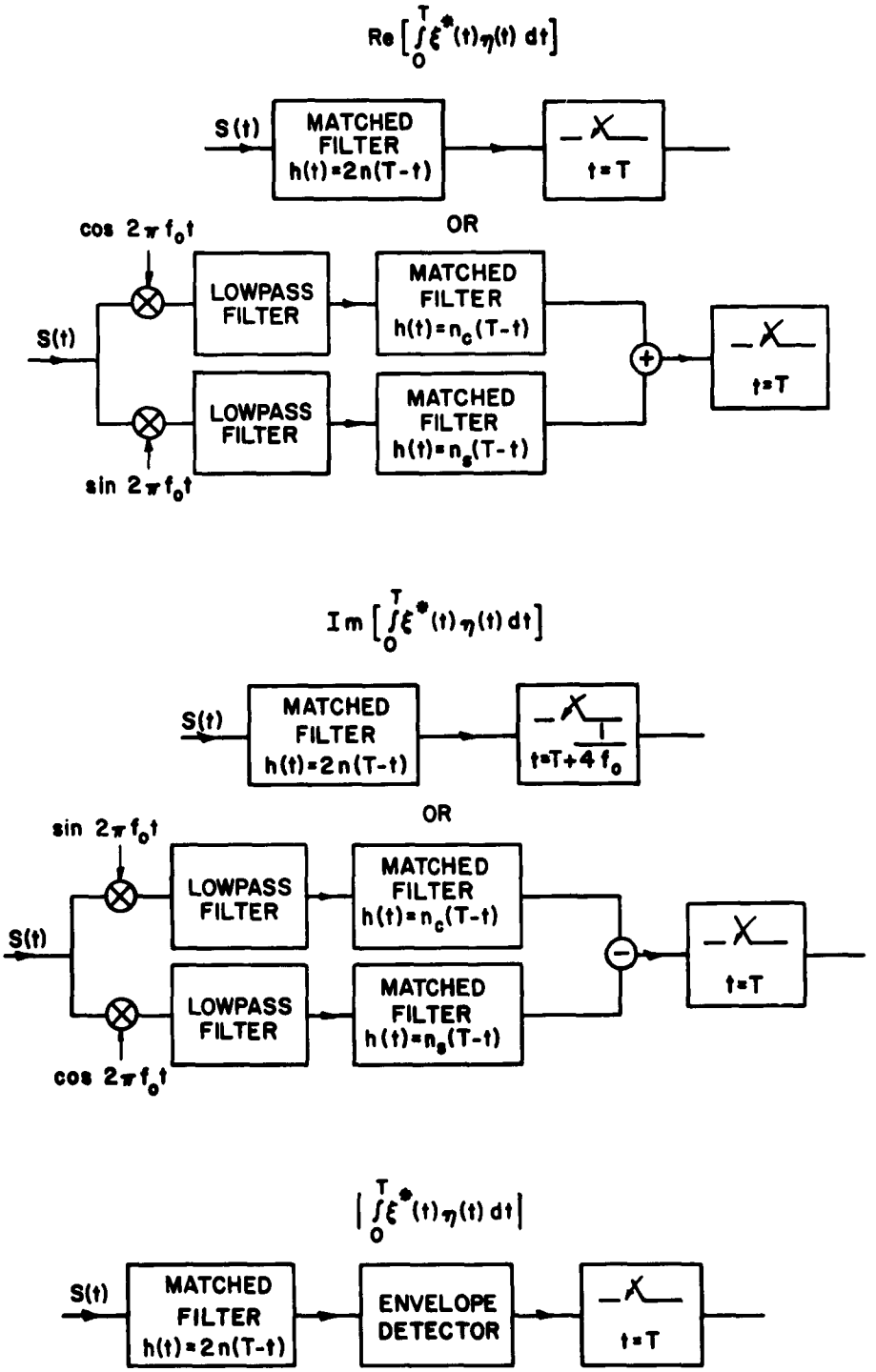

Fig. 35. Computation of correlation integrals by matched filters.

One way of computing these integrals is by using the matched filters of Fig. 35.

Thus far, we have considered only waveforms for which the Fourier transforms exist. If we deal with narrow-band random processes, it can be shown that exactly the same representation holds in a limit-in-the-mean sense.

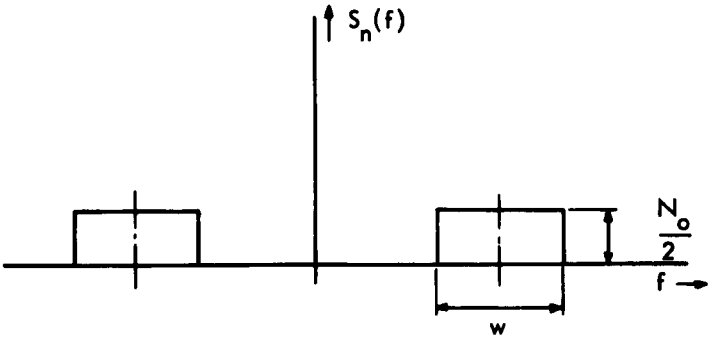

Fig. 36. Power spectral density of bandlimited white noise.

If, for instance, we have white bandlimited noise with power density N_o(watts/cps) over a bandwidth W such as that in Fig. 36, its quadrature components are independent lowpass functions with zero mean and identical autocorrelation functions.

$$R_{n_s}(\tau) = R_{n_c}(\tau) = WN_o \frac{\sin \pi W\tau}{\pi W\tau} \quad . \tag{67}$$

4.3 COMPUTATION OF PROBABILITIES

Our communication system is of the type pictured in Fig. 3 in which the notation now indicates complex waveforms. According to statistical decision theory, the optimum receiver computes the set of a posteriori probabilities $P(\xi_m(t)/\zeta(t))$ in order to make its decision. As was briefly mentioned in Section I, this is equivalent to computing the set of likelihoods

$$\Lambda_m \sim p(\zeta(t)/\xi_m(t))$$

for every possible waveform. We shall now consider the operations involved in more detail.

a. The "Likelihoods"

Our channel model is very similar to that of Turin[21] and we are going to use essentially the same technique to obtain the receiver structure.

Using the notations given in Fig. 3, we transmit a certain waveform

$$\xi_m(t) = x_m(t)\, e^{j\omega_o t} \qquad 0 \leq t \leq T. \tag{68}$$

Depending on the multipath structure, the output of the random filter is

$$\nu_m(t) = \sum_{i=1}^{L} a_i \, x_m(t-\tau_i) \exp[j(\omega_o t - \theta_i)], \tag{69}$$

where a_i, θ_i and τ_i are the amplitude, phase shift, and delay associated with a particular path. White Gaussian noise is added to the output of the random filter so that what is actually received is

$$\zeta(t) = \nu_m(t) + \eta(t) = z(t) \exp(j\omega_o t). \tag{70}$$

According to our assumptions, the receiver knows the delay and has estimates of the amplitude and phase for every one of the L paths. We assume that the paths are varying slowly enough so that these parameters can be considered as constants during the reception of a waveform. Let us denote the actual amplitude and phase of the L paths by the vectors

$$\bar{a} = (a_1, a_2, \ldots, a_L)$$

$$\bar{\theta} = (\theta_1, \theta_2, \ldots, \theta_L).$$

We then have a probability density of 2L variables for the occurence of a particular set of $\bar{a}$ and $\bar{\theta}$. Since we probably can assume that the estimation errors are stationary with zero mean, we have the same shape distribution but with different means from decision to decision.

To obtain the "likelihood" under the assumption that the m^{th} waveform was sent, we first calculate the conditional probability density for a particular set of channel parameters. Using the fact that the additive noise is white and Gaussian, we can show that

$$\Lambda_{\bar{a},\bar{\theta}} = p(\zeta(t)/\bar{a},\bar{\theta}) = \text{constant} \exp\left(-\frac{1}{2N_o} \int_0^{T_d} |\zeta(t)-\nu_m(t)|^2 \, dt\right), \tag{71}$$

where N_o is the noise power per cycle (cf. Fig. 36) and T_d is the duration of the received signal. We multiply (71) by the probability density for the channel parameters and integrate, which gives

$$\Lambda = \text{const.} \int_{-\infty}^{\infty} \cdots \int_{-\infty}^{\infty}_{2L} \exp\left(-\frac{1}{2N_o} \int_0^{T_d} |\zeta(t)-\nu_m(t)|^2 \, dt\right) p(\bar{a},\bar{\theta}) \, d\bar{a} \, d\bar{\theta}, \tag{72}$$

where $d\bar{a}\, d\bar{\theta}$ denotes $da_1, \ldots, da_L \, d\theta_1, \ldots, d\theta_L$.

$$\int_0^{T_d} |\zeta(t)-\nu_m(t)|^2 \, dt = \int_0^{T_d} |\zeta(t)| \, dt - \int_0^{T_d} \zeta(t) \, \nu_m^*(t) + \zeta^*(t) \, \nu_m(t) \, dt$$

$$+ \int_0^{T_d} |\nu_m(t)|^2 \, dt. \tag{73}$$

The first term $\int |\zeta(t)|\, dt$ is not dependent on the index m or the integration variables, and we can incorporate it into the constant in front of Λ. The last term does not depend on the received waveform and the second term can be written by using the complex notation in (69) and (70)

$$\int_0^{T_d} [\zeta(t)\, \nu_m^*(t) + \zeta^*(t)\, \nu_m(t)]\, dt = 2 \sum a_i [U_{mi} \sin \theta_i + V_{mi} \cos \theta_i], \tag{74}$$

where

$$\left.\begin{aligned} U_{mi} &= \mathrm{Im} \\ V_{mi} &= \mathrm{Re} \end{aligned}\right\} \int_0^{T_d} z^*(t)\, x_m(t-\tau_i)\, dt.$$

The correlation integrals U_m and V_m can also be written as given in (64) and (65), and according to Fig. 35 we can compute them by passing the received wave through a filter matched to the transmitted waveform. Notice that we need (at least in principle) only one filter for each index m; all of the U_{mi} and V_{mi} (i=1, 2, . . . , L) can be obtained by sampling the output from the matched filter at the right instant of time.

The decision procedure thus is to compute the set of correlation terms U_{mi} and V_{mi} (i=1, 2, . . . , L) for each possible waveform and then combine these terms to get the "likelihood" function Λ. U and V are sufficient statistics in the sense that they contain all of the information about the received waveform that is needed to make the decision. To proceed further, we now make the assumption that the transmitted waveforms have correlation functions that are narrow compared with the delay between paths. This means that

$$\psi_m(\tau) = \int_0^T x_m^*(t)\, x_m(t-\tau)\, dt \cong 0 \qquad \text{for } \tau = \tau_i - \tau_j \text{ all m and } i, j = 1, \ldots, L. \tag{75}$$

If we also assume that all transmitted waveforms have the same energy,

$$2E = \int_0^T |x_m(t)|^2\, dt \qquad \text{all m,} \tag{76}$$

we can write

$$\int_0^{T_d} |\nu_m(t)|^2\, dt = \int_0^{T_d} \sum_i \sum_j a_i a_j x_m(t-\tau_i)\, x_m^*(t-\tau_j)\, dt \cong 2E \sum_i^L a_i^2. \tag{77}$$

The exponential in (72) now factors into a product of terms. If the paths are statistically independent, we can also factor the probability density and we have

$$\ln \Lambda_m = C + \sum_{i=1}^{L} \ln \int_{-\infty}^{\infty} \exp\left(\frac{a_i}{N_o}(U_{mi} \sin\theta_i + V_{mi} \cos\theta_i) - \frac{E}{N_o} a_i^2\right) p_i(a_i, \theta_i)\, da_i\, d\theta_i$$

$$= C + \sum_{i=1}^{L} W_i(U_{mi}, V_{mi}). \tag{78}$$

We see that under these assumptions we can weight the contribution from each path separately. The weighting functions W_i depend on the distribution of the path parameters, but not on the signal index m. The variables in the weighting functions U and V are random variables and their distribution depends on the channel variation, the noise, and the particular waveform that was actually transmitted.

b. Distribution for the Sufficient Statistics U and V

As we have pointed out, U and V contain all of the information that the receiver needs to make its decision, and a simple way of computing them is by filters matched to the possible transmitted waveforms.

To evaluate U_{mi} and V_{mi} when the waveform with index k was sent, we write

$$\left.\begin{matrix} U_{mi/k} = \text{Im} \\ V_{mi/k} = \text{Re} \end{matrix}\right\} \int_0^{T_d} \left(\sum_{i=1}^{L} a_i x_k^*(t-\tau_i)\, e^{j\theta i} + n^*(t) \right) x_m(t-\tau_i)\, dt. \tag{79}$$

We have assumed that the transmitted waveforms had narrow correlation functions. We now make the additional assumption that the crosscorrelation between signals is small for shifts corresponding to the differences in path delays.

$$\psi_{mk}(\tau) = \int_0^T x_m^*(t)\, x_k(t-\tau)\, dt \cong 0 \qquad \begin{matrix} \text{for } \tau = \tau_i - \tau_j \\ i, j = 1, 2, \ldots, L \\ \text{all m and k} \end{matrix} \tag{80}$$

We need then consider only one term in the sum in (79) which gives

$$U_{mi/k} = a_i [E_{km}^{(c)} \sin\theta_i + E_{km}^{(s)} \cos\theta_i] + \text{Im} \int_0^{T_d} n^*(t)\, x_m(t-\tau_i)\, dt \tag{81}$$

$$V_{mi/k} = a_i [E_{km}^{(c)} \cos\theta_i - E_{km}^{(s)} \sin\theta_i] + \text{Re} \int_0^{T_d} n^*(t)\, x_m(t-\tau_i)\, dt, \tag{82}$$

where $E_{km}^{(c)}$ and $E_{km}^{(s)}$ denote the real and imaginary parts of the complex crosscorrelation between signals:

$$E_{km}^{(c)} = \text{Re} \int_0^T x_k^*(t)\, x_m(t)\, dt = \int_0^T x_{ck}(t)\, x_{cm}(t) + x_{sk}(t)\, x_{sm}(t)\, dt \tag{83}$$

$$E_{km}^{(s)} = \text{Im} \int_0^T x_k^*(t)\, x_m(t)\, dt = \int_0^T x_{ck}(t)\, x_{sm}(t) - x_{sk}(t)\, x_{cm}(t)\, dt, \tag{84}$$

Since we assume that the noise is independent of the channel, we can consider $U_{mi/k}$ and $V_{mi/k}$ as the sum of two independent random variables.

$$U_{mi/k} = u_{mi/k} + u_n \tag{85}$$

$$V_{mi/k} = v_{mi/k} + v_n. \tag{86}$$

The noise is Gaussian and u_n and v_n are obtained by a linear operation on the noise, so they are Gaussian variables with mean, variance, and covariance given by

$$E[u_n] = E[v_n] = 0 \tag{87}$$

$$E[u_n^2] = E[v_n^2] = 2N_oE \tag{88}$$

$$E[u_n v_n] = 0, \tag{89}$$

where E is given by (76).

Hence u_n and v_n are independent Gaussian variables with zero mean and equal variance, independent of the indices m and k. By using Eq. 80, it is easy to show that the distribution is also independent of the path index i. The remaining terms $u_{mi/k}$ and $v_{mi/k}$ are linear combinations of the channel parameters, and we can write

$$u_{mi/k} = E_{km}^{(c)}\, x_i + E_{km}^{(s)}\, y_i \tag{90}$$

$$v_{mi/k} = E_{km}^{(c)}\, y_i - E_{km}^{(s)}\, x_i. \tag{91}$$

Here, we have written the channel parameters in Cartesian coordinates.

$$x_i = a_i \sin \theta_i \tag{92}$$

$$y_i = a_i \cos \theta_i. \tag{93}$$

Equations 90 and 91 correspond to a rotation and linear scaling of the variables x_i and y_i; this means that the joint distribution of $u_{mi/k}$ and $v_{mi/k}$ has the same form as the distribution of x_i and y_i apart from the direction of the coordinate axis and a scale factor.

Let us define a new pair of variables by the rotational transformation.

$$u'_{mi/k} = \frac{1}{\beta_{km}} \left[E_{km}^{(s)}\, u_{mi/k} - E_{km}^{(c)}\, v_{mi/k}\right] \tag{94}$$

$$v'_{mi/k} = \frac{1}{\beta_{km}} \left[E_{km}^{(c)}\, u_{mi/k} + E_{km}^{(s)}\, v_{mi/k}\right], \tag{95}$$

where $\beta_{km} = \sqrt{\left(E_{km}^{(s)}\right)^2 + \left(E_{km}^{(c)}\right)^2}$. We then have

$$u'_{mi/k} = \beta_{km} x_i$$

$$v'_{mi/k} = \beta_{km} y_i$$

which gives

$$p_{u', v}(r, s) = \frac{1}{\beta_{km}^2} p_{x_i, y_i}\left(\frac{r}{\beta}, \frac{s}{\beta}\right). \tag{96}$$

This connection between the two distriubtions is illustrated in Fig. 37. Equation 96 gives the distribution for the part of U and V that depends on the channel. To get the

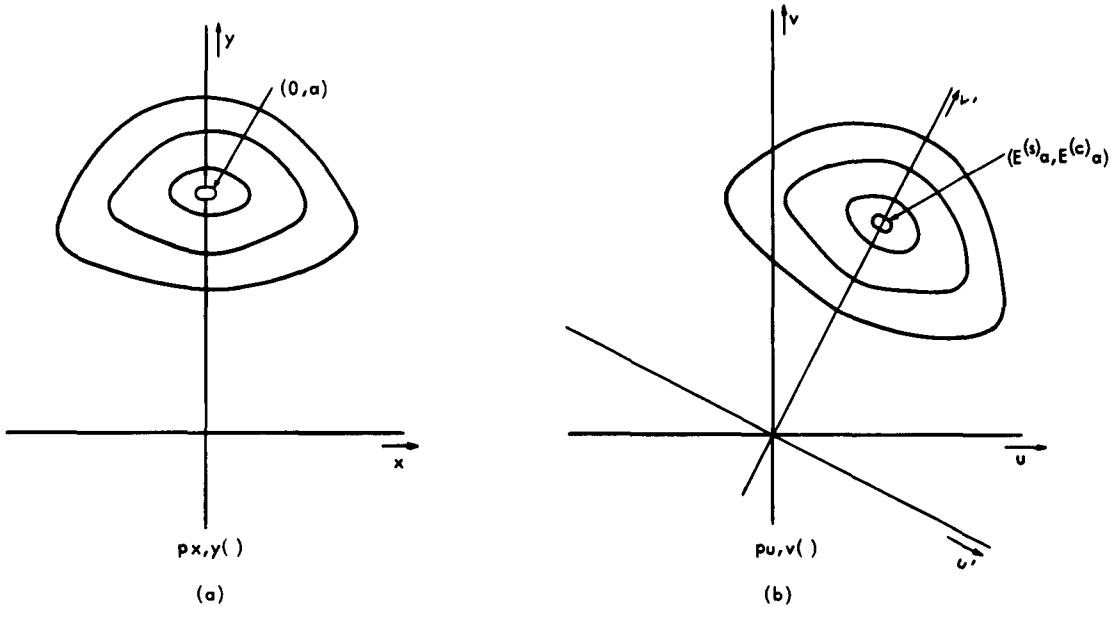

Fig. 37. Probability density functions. (a) Distribution for path parameters. (b) Distribution for decision variables.

distribution for U and V themselves, we have to add the part corresponding to the noise. Adding independent variables corresponds to taking the convolution of the probability densities, and we finally have the joint distribution for U and V.

$$p_{U, V}(u', v') = \int_{-\infty}^{\infty} \int_{-\infty}^{\infty} \frac{1}{\beta^2} p_{x_i, y_i}\left(\frac{r}{\beta}, \frac{s}{\beta}\right) \frac{1}{2\pi N_o E} \exp\left(-\frac{(u'-r)^2+(v'-s)^2}{2N_o E}\right) dr\, ds. \tag{97}$$

To simplify our discussion, let us assume that the probability density for the channel parameters is symmetrical around some axis. We can assume symmetry around the

y-axis, since a rotation of the xy-axis corresponds to an identical rotation of the UV-axis. We then have

$$E[x_i] = 0$$

$$E[y_i] = a_i$$

$$E\left[x_i^2\right] = \sigma_{x_i}^2$$

$$E[(y_i - a_i)^2] = \sigma_{y_i}^2.$$

It is convenient to introduce new normalized variables

$$U^o_{mi/k} = \frac{U_{mi/k}}{\sigma_{y_i}\sqrt{2E}}; \quad V^o_{mi/k} = \frac{V_{mi/k}}{\sigma_{y_i}\sqrt{2E}} \tag{98}$$

$$x_i^o = \frac{x_i}{\sigma_{y_i}}; \quad y_i^o = \frac{y_i}{\sigma_{y_i}}. \tag{99}$$

The signal power at the transmitter has no real significance, since we can have a gain or attenuation in the channel and we therefore define a signal-to-noise ratio at the receiver

$$d_i^2 = \frac{\sigma_{x_i}^2 + \sigma_{y_i}^2 + a_i^2}{N_o} E. \tag{100}$$

Clearly, d_i^2 is the average signal power for the i^{th} path at the receiver divided by the noise power density. We define two other quantities

$$c_a = \frac{a}{\sigma_y} \tag{101}$$

$$C_\phi = \sigma_x/\sigma_y. \tag{102}$$

Since a is the nonrandom part of the path strength, c_a is a measure of the uncertainty in path strength. Similarly, c_ϕ can be considered as a measure of the uncertainty of phase.

$$E\left[x_i^o\right] = 0; \quad E\left[y_i^o\right] = c_a \tag{103}$$

$$E\left[x_i^{o2}\right] = c_\phi^2; \quad E[(y_i^o - c_a)^2] = 1 \tag{104}$$

Then, under the assumption that x_i and y_i are independent, we obtain for the mean and variance of our normalized decision variables

$$E[U^{o}_{mi/k}] = \frac{E^{(s)}_{km}}{2E} c_{a_i} \tag{105}$$

$$E[V^{o}_{mi/k}] = \frac{E^{(c)}_{km}}{2E} c_{a_i} \tag{106}$$

$$\sigma^2[U^{o}_{mi/k}] = \left(\frac{E^{(c)}_{km}}{2E}\right)^2 c^2_{\phi_i} + \left(\frac{E^{(s)}_{km}}{2E}\right)^2 + \frac{c^2_{\phi_i} + c^2_{a_i} + 1}{2d^2_i} \tag{107}$$

$$\sigma^2[V^{o}_{mi/k}] = \left(\frac{E^{(s)}_{km}}{2E}\right)^2 c^2_{\phi_i} + \left(\frac{E^{(c)}_{km}}{2E}\right)^2 + \frac{c^2_{\phi_i} + c^2_{a_i} + 1}{2d^2_i} \tag{108}$$

When we test the hypothesis that the k^{th} waveform was transmitted we have

$$E^{(s)}_{kk} = 0, \quad E^{(c)}_{kk} = 2E$$

$$E[U^{o}_{ki/k}] = 0$$

$$E[V^{o}_{ki/k}] = c_{a_i} \tag{109}$$

$$\sigma^2[U^{o}_{ki/k}] = c^2_{\phi_i} + \frac{c^2_{\phi_i} + c^2_{a_i} + 1}{2d^2_i} \tag{110}$$

$$\sigma^2[V^{o}_{ki/k}] = 1 + \frac{c^2_{\phi_i} + c^2_{a_i} + 1}{2d^2_i} \cdot \tag{111}$$

The probability density for the normalized decision variables under the hypothesis that the correct waveform was sent is identical with the normalized density for the channel with the addition of Gaussian noise. We know that the other decision variables have the same type of distribution but centered around other points in the $U^{o}V^{o}$-plane and depending on the crosscorrelation between signals. For the important special case for which all signals are orthogonal, i. e.,

$$E^{(s)}_{km} = E^{(c)}_{km} = 0 \qquad \text{all } k \neq m$$

we have

$$E[U^{o}_{mi/k}] = E[V^{o}_{mi/k}] = 0 \tag{112}$$

$$\sigma^2[U^o_{mi/k}] = \sigma^2[V^o_{mi/k}] = \frac{c^2_{\phi_i} + c^2_{a_i} + 1}{2d_i^2} \qquad m \neq k \tag{113}$$

which is a symmetrical Gaussian distribution around the origin. The decision variables for different hypotheses are in general statistically dependent but in the case of orthogonal signals they are independent.

c. The Weighting Function $W_i(U, V)$

We have seen that the distribution for the decision variables U and V is closely related to the distribution of the channel parameters. The weighting function given by (78) represents the weight that should be put on the U and V connected with a particular path. It is still convenient to work with normalized variables. Substituting Eqs. 92, 93, 98, and 99 in (78), we get

$$W_i(U^o, V^o) = \ln \int_{-\infty}^{\infty} \int_{-\infty}^{\infty} \exp\left\{\frac{\sigma_y^2 E}{N_o}[2U^o x + 2V^o y - x^2 - y^2]\right\} p_i^o(x, y)\, dx\, dy, \tag{114}$$

where $P_i^o(x, y)$ denotes the density function normalized according to (103) and (104). It is in general not possible to solve the integral in (114) and obtain W(U, V) in closed form; nevertheless, it is possible to determine certain properties of it. In Appendix D we prove that W(U, V) has a minimum at a finite point in the UV-plane unless the whole probability mass of $P_i^o(x, y)$ is located in a half-plane. Its second differential is always positive which means that the function is monotonically increasing from the minimum point in all directions. If P(x, y) has a symmetry line through the origin in the xy-plane, W(U, V) is symmetric around the same line in the UV-plane.

To illustrate the connections between the different concepts involved, we work out in detail the case in which the channel parameters x_i and y_i have a joint Gaussian distribution. With

$$p_i^o(x, y) = \frac{1}{2\pi c_{\phi_i}} \exp\left(-\frac{\left(y - c_{a_i}\right)^2}{2}\right) \exp\left(-\frac{x^2}{2c^2_{\phi_i}}\right)$$

we easily obtain, by completing the squares in the exponent in (114),

$$W_i(U^o, V^o) = \frac{U^{o2}}{a_i^2} + \frac{\left(V^o + \frac{c_{a_i}}{e_i}\right)^2}{b_i^2} - \frac{c_a^2}{2} - \frac{1}{2}\ln\left[(e_i+1)\left(e_i c^2_{\phi_i} + 1\right)\right], \tag{115}$$

where

$$e_i = \frac{2\sigma_{y_i}^2 E}{N_o} = \frac{2d_i^2}{1 + c_{\phi_i}^2 + c_{a_i}^2} \tag{116}$$

$$a_i = \frac{\sqrt{2e_i c_{\phi_i}^2 + 1}}{e_i c_{\phi_i}} \tag{117}$$

$$b_i = \frac{\sqrt{2e_i + 1}}{e_i}. \tag{118}$$

Here, c_{a_i}, c_{ϕ_i} and d_i are the normalization parameters defined in (100)-(102). We see that W(U, V) is an elliptic paraboloid centered around the point $-c_{a_i}/e_i$ on the V-axis. The decision variables in this case are all independent Gaussian variables if we assume orthogonal signals.

$$p_{U^o_{k/k'}, V^o_{k/k}}(U, V) = \frac{1}{2\pi\sqrt{c_{\phi_i}^2 + 1/e_i}} \exp\left(-\frac{U^2}{2\left(c_{\phi_i}^2 + 1/e_i\right)}\right)$$

$$\times \frac{1}{\sqrt{1 + 1/e_i}} \exp\left(-\frac{\left(V - c_{a_i}\right)^2}{2(1+1/e_i)}\right) \tag{119}$$

$$p_{U^o_{m/k'}, V^o_{m/k}}(U, V) = \frac{e_i}{2\pi} \exp\left(-\frac{U^2}{2/e_i}\right) \exp\left(-\frac{V^2}{2/e_i}\right). \tag{120}$$

For the special case in which $c_{\phi_i} = 1$, W(U, V) is a circular paraboloid and the distribution for the channel parameters is Rician (cf. Eq. 8) for the amplitude. In Fig. 38 this situation is pictured for a certain signal-to-noise ratio. The probability densities of U and V for the correct and incorrect waveforms are drawn in the same graph as W(U, V). To minimize the probability of errors, these two probability densities should be placed as far apart as possible in the paraboloid. Since the location of the distribution for the incorrect waveforms depends on the crosscorrelation between the signals, it is in general advantageous to use signals with a negative crosscorrelation: $E_{km} < 0$. If we use the prediction procedure outlined in Section III, there is no special reason to expect the statistics of the channel to be Rician. Since we estimate amplitude and phase separately, it seems more likely to get independent, approximately Gaussian errors in amplitude and phase which correspond to a distribution of the type given in Fig. 37. On the contrary,we have seen that the general character of W(U, V) as a "bowl" is independent of the shape of the channel distribution. It therefore seems plausible that the

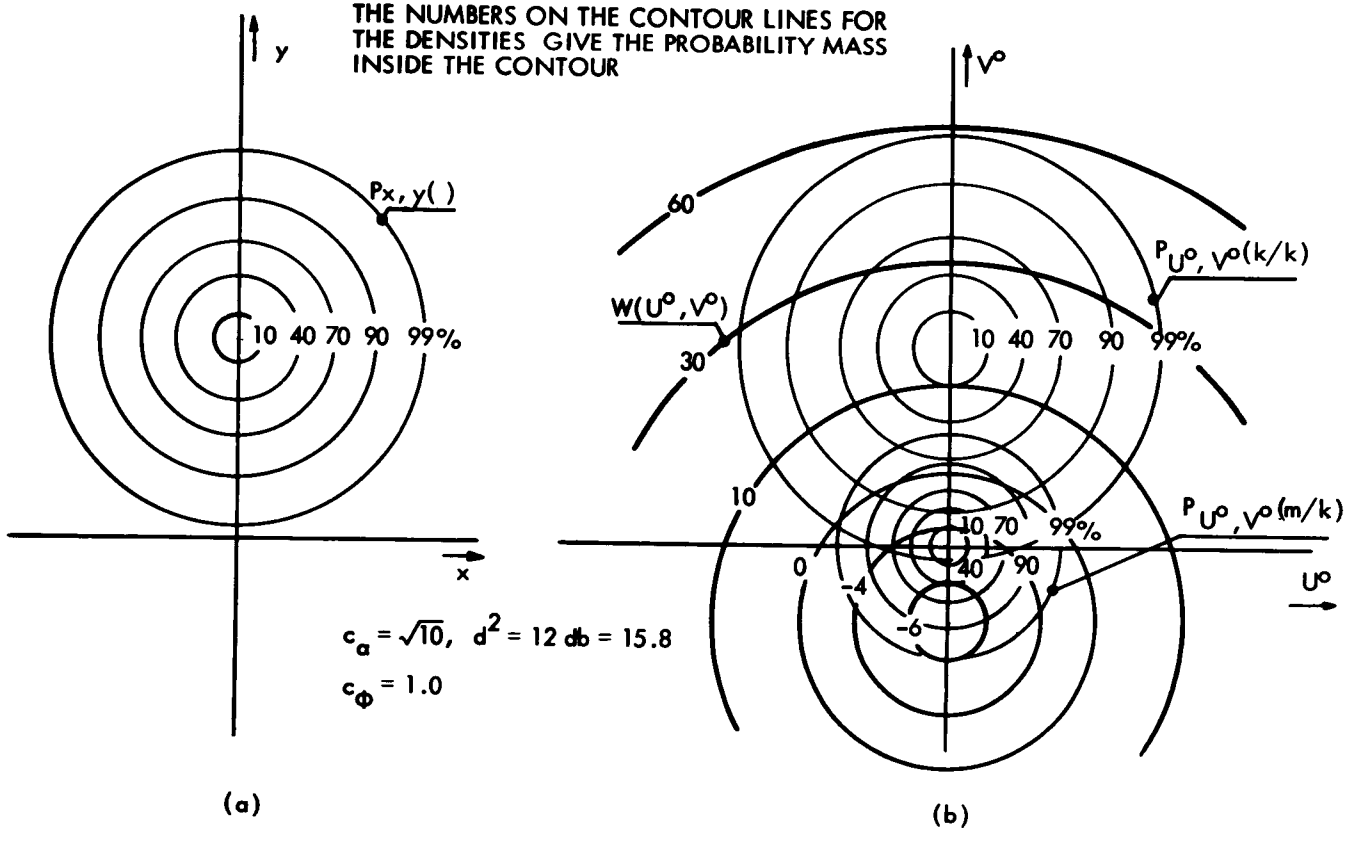

Fig. 38. Probability densities and weighting function. (a) Channel distribution. (b) Weighting function and distributions for decision variables.

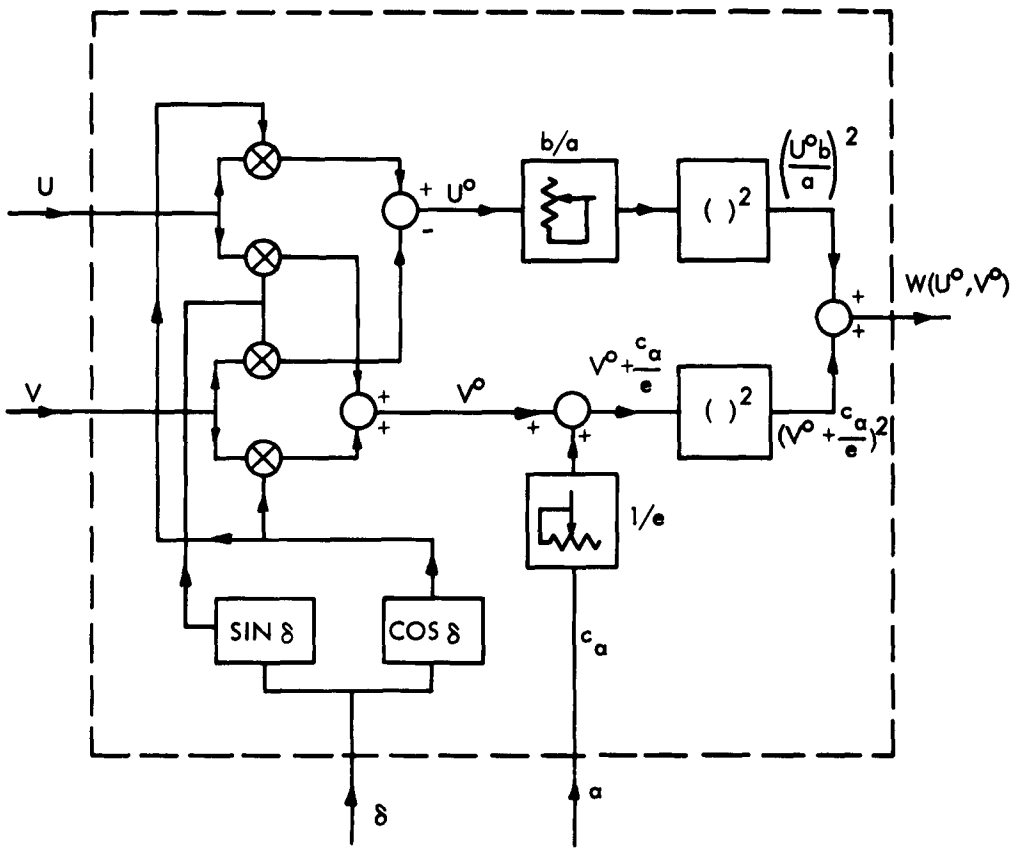

Fig. 39. Block diagram for the weighting function W(U, V) (Modified Rician Case).

decision function will work well for any probability density that has the form of a single "hill." By choosing $c_\phi > 1$, we get a distribution with larger uncertainty in phase than the Rician distribution, which perhaps corresponds better to the real situation.

To arrive at the form of W(U, V) in (115), we made the assumption that the channel distribution was centered around the y-axis as in Fig. 38a, which is for zero phase. In general, we have an estimate of the phase shift different from zero, but it is easy to take into account by "rotation" of the UV-plane, since a rotational transformation of x and y corresponds to an identical transformation of U and V. The last term in (115) is a constant and we can simply ignore it when we form the "likelihoods" (78). To compute the rest of W(U, V) we can, for instance, use the diagram in Fig. 39.

d. Receiver Block Diagram

The receiver structure can be summarized as follows. Compute the decision variables U and V for each possible waveform. Combine the U and V for a particular path, using the available knowledge about the amplitude and phase of that path. By adding the W(U, V) for each path, the likelihoods are obtained and further decision depends on

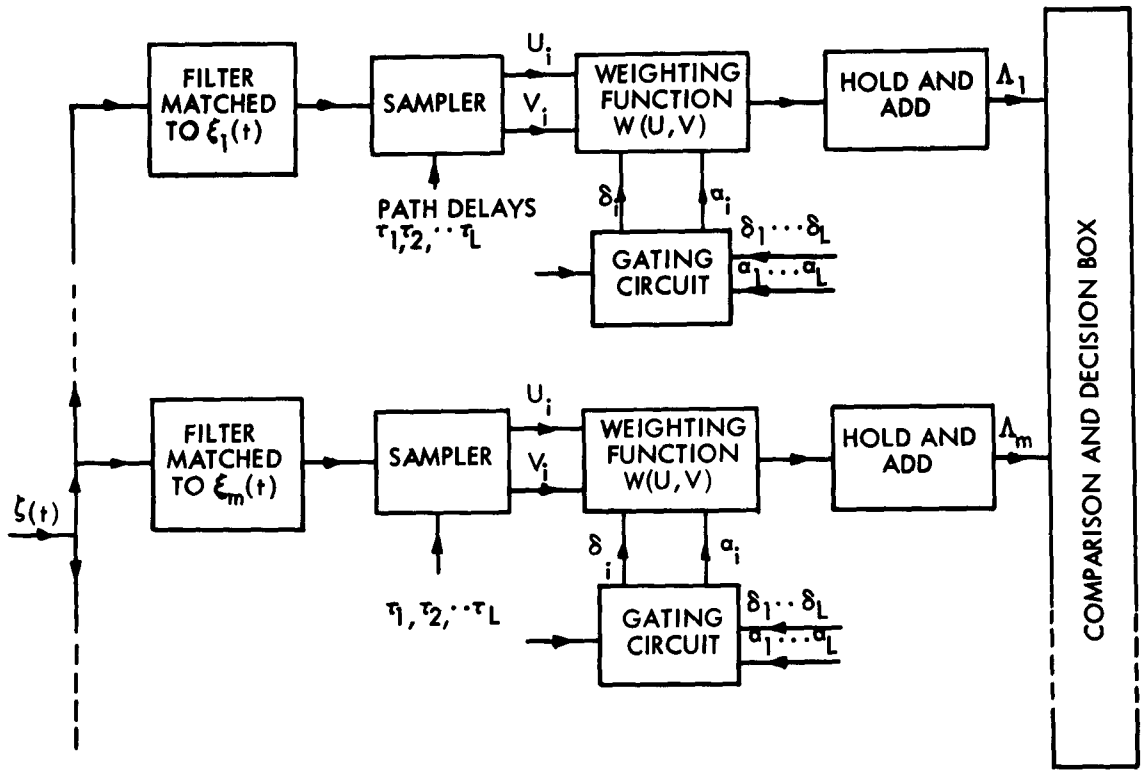

Fig. 40. Receiver block diagram.

a priori probabilities and costs, or on some other criteria that depend on the practical situation.

There is no reason to suspect that the statistics for different paths should differ in general character and it should, therefore, be possible to use the same weighting function for all of them. We have pointed out that all of the U and V corresponding to a particular waveform could be obtained by sampling a matched filter at times corresponding to the path delay. We can by proper gating use the same weighting box for all of the paths and have the receiver shown in Fig. 40.

4.4 DISCUSSION

The receiver structure that we have obtained is not too complicated. It consists basically of a set of matched filters, one for each possible waveform. By weighting the outputs from the filters corresponding to different paths properly, the "likelihoods" for each waveform are formed. The form of the weighting function was derived for the case of a "modified Rician" distribution for the paths. It has been shown that the weighting function is not sensitive to the detailed form of the path statistics, and it seems likely that the derived function should work well even for other reasonable statistics.

It should be emphasized that certain assumptions about the transmitted waveforms

were made in order that the mathematics be tractable. We assumed that there is no overlap between different signals caused by the multipath and that the waveforms have narrow correlation functions compared with the time delay between paths. These assumptions make it possible for the receiver to separate the parts of the received signal for different paths. We can say that the multipath structure is used to obtain independent copies of the transmitted signal disturbed by noise, and, in principle, we have the same situation as that for diversity reception.

The probability of error is determined by the distribution of the decision variables U and V, under different hypotheses as to which waveform was actually transmitted. Turin[22] has computed the error probability for a single Rician path when only two orthogonal signals are used, and his results are directly applicable to our receiver.

It is well known that the detection probability for signals of random phase is not much less than that for completely known signals when the signal-to-noise ratio is high. See, Helstrom,[10] for instance. On the other hand, when the path strength is weak, and hence the signal-to-noise ratio low, our receiver cannot obtain a reliable estimate of the phase, and the decision is made mainly on the envelope of the received signal. The question arises if the gain obtained by estimating the phase is significant in terms of probability of error or signal-to-noise ratio. If it turns out that it is not worth while to estimate the phase, we must question whether there is any real need for information about the path strength. If only one path is present, this is clearly not the case, and if we have several paths, we use the estimate of the path strength only to properly combine the decision variables corresponding to different paths. As we have pointed out, our receiver is very similar to a diversity combiner, and (as shown by Brennan[5]) the difference in performance between different diversity techniques, with or without knowledge of the actual signal strength, is not great. If neither phase nor amplitude for the paths need be estimated, the only knowledge the receiver needs about the multipath structure is the path delays.

Many important questions need to be answered before claims can be made about the practical value of a communication system such as the one outlined in this report. Nevertheless, our model provides a way of supplying the receiver with knowledge about the random channel in a way that it is possible to analyze mathematically, and the results obtained should give insight into the problem of what can be achieved by applying statistical communication theory to a multipath medium.

APPENDIX A

Sampling Theorem for Time-Variant Filters

Assume that we have a linear time-variant filter which we characterize by its response function

$h(y, t)$ = response at time t of an impulse applied at time $t-y$.

For an input $u(t)$ we then have the output $v(t)$

$$v(t) = \int_{-\infty}^{\infty} h(y, t)\, u(t-y)\, dy. \tag{A-1}$$

For a realizable filter $h(y, t) = 0$ for $y < 0$.

We can define a corresponding frequency function

$$H(jf, t) = \int_{-\infty}^{\infty} h(y, t)\, e^{-j2\pi fy}\, dy \tag{A-2}$$

$H(jf, t)$ is the Fourier transform of $h(y, t)$ with t treated as a constant, and we can make the physical interpretation

$$H(jf, t) = \frac{\text{Response to } e^{j2\pi ft}}{e^{j2\pi ft}} \tag{A-3}$$

If $u(t)$ is a bandpass signal, $f_c - \frac{W}{2} \leq |f| \leq f_c + \frac{W}{2}$, we can put an ideal bandpass filter before our time-variant filter without changing anything (see Fig. 9). Thus

$$v(t) = \int_{-\infty}^{\infty} h'(y, t)\, u(t-y)\, dy \qquad u(t) \text{ bandlimited} \tag{A-4}$$

Here, we consider the cascade of the bandpass filter and our original filter as a new filter with response function $h'(t, y)$. The corresponding frequency function is

$$H'(jf, t) \begin{cases} = H(jf, t) & f_c - \frac{W}{2} \leq |f| \leq f_c + \frac{W}{2} \\ = 0 & \text{otherwise} \end{cases} \tag{A-5}$$

and we can write

$$h'(y, t) = \int_{-f_c - \frac{W}{2}}^{-f_c + \frac{W}{2}} e^{j2\pi fy} \left(\int_{-\infty}^{\infty} h(y, t)\, e^{-j2\pi fy}\, dy \right) df$$

$$+ \int_{f_c - \frac{W}{2}}^{f_c + \frac{W}{2}} e^{j2\pi fy} \left(\int_{-\infty}^{\infty} h(y, t)\, e^{-j2\pi fy}\, dy \right) df \tag{A-6}$$

The Fourier transform of $h'(t, y)$ with respect to y is bandlimited for all t and we can apply a sampling theorem. Using the notations of Woodward,[24] we have

$$h'(y, t) = \sum_{n=-\infty}^{\infty} h'\left(\frac{n}{w}, t\right) \text{sinc } w\left(y-\frac{n}{w}\right) \cos 2\pi f_c \left(y-\frac{n}{w}\right)$$

$$- \sum_{n=-\infty}^{\infty} \hat{h}'\left(\frac{n}{w}, t\right) \text{sinc } w\left(y-\frac{n}{w}\right) \sin 2\pi f_c \left(y-\frac{n}{w}\right), \qquad \text{(A-7)}$$

where $\hat{h}$ denotes Hilbert transform with respect to y and $\text{sinc } x = \frac{\sin \pi x}{\pi x}$ (see Woodward[24] for a derivation). Substituting (A-7) in (A-4), we get

$$v(t) = \sum_{n=-\infty}^{\infty} h'\left(\frac{n}{w}, t\right) \int_{-\infty}^{\infty} \text{sinc } w\left(y-\frac{n}{w}\right) \cos 2\pi f_c \left(y-\frac{n}{w}\right) u(t-y)\, dy$$

$$- \sum_{n=-\infty}^{\infty} \hat{h}'\left(\frac{n}{w}, t\right) \int_{-\infty}^{\infty} \text{sinc } w\left(y-\frac{n}{w}\right) \sin 2\pi f_c \left(y-\frac{n}{w}\right) u(t-y)\, dy \qquad \text{(A-8)}$$

By changing the variables of integration the integrals can be written as

$$I_{cn}(t) = u\left(t-\frac{n}{w}\right) * \text{sinc } wt \cdot \cos 2\pi f_c t \qquad \text{(A-9)}$$

$$I_{sn}(t) = u\left(t-\frac{n}{w}\right) * \text{sinc } wt \cdot \sin 2\pi f_c t, \qquad \text{(A-10)}$$

where * denotes convolution.

The Fourier transform of $\text{sinc } wt \cdot \cos 2\pi f_c t$ is

$$\mathcal{F}[\text{sinc } wt \cdot \cos 2\pi f_c t] = \frac{1}{2w}\left[\text{rect}\left(\frac{f-f_c}{w}\right) + \text{rect}\left(\frac{f+f_c}{w}\right)\right] \qquad \text{(A-11)}$$

$$\text{rect } x \begin{cases} = 1 & |x| < 1/2 \\ = 0 & |x| > 1/2 \end{cases}$$

Since convolution in time corresponds to multiplication in the frequency domain we realize that $I_{cn}(t)$ corresponds to passing $u\left(t-\frac{n}{w}\right)$ through the bandpass filter in Fig. A-1. According to our assumptions $u(t)$ has no frequency components outside the passband of this filter and we simply have

$$I_{cn}(t) = \frac{1}{2w} u\left(t-\frac{n}{w}\right) \qquad \text{(A-12)}$$

In a completely analogous way we obtain the result that $I_{sn}(t)$ corresponds to passing $u\left(t-\frac{n}{w}\right)$ through the filter in Fig. A-2. This is simply a Hilbert transforming filter for

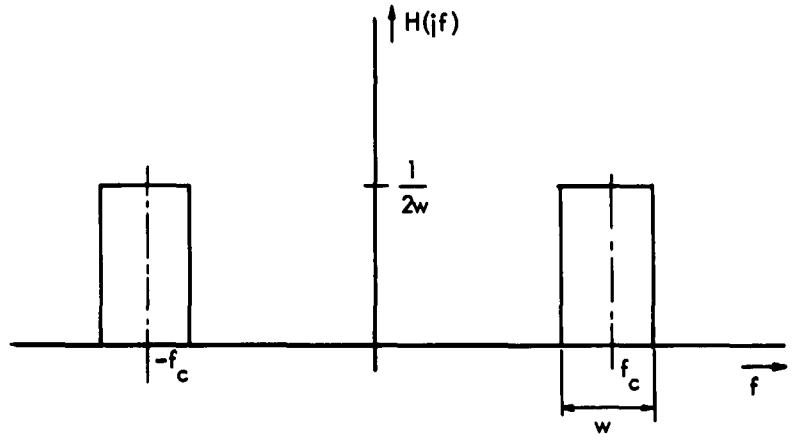

Fig. A-1. Ideal bandpass filter.

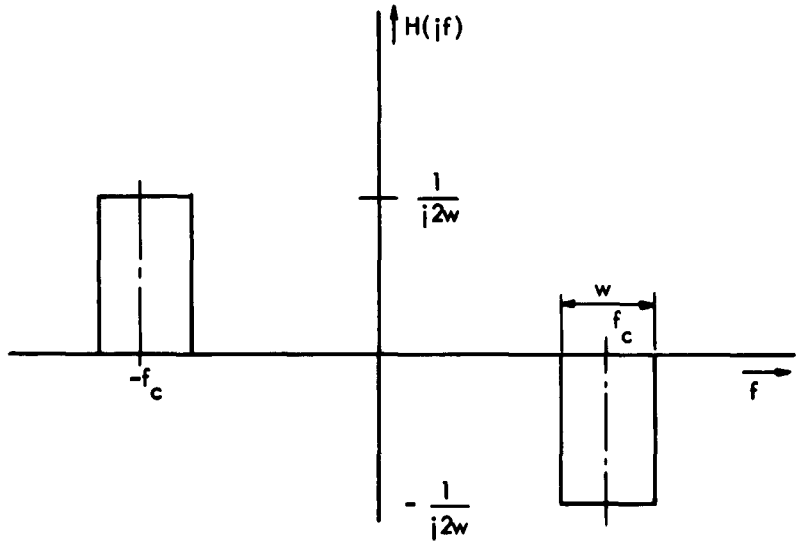

Fig. A-2. Hilbert transforming bandpass filter.

bandpass functions and we have

$$I_{sn}(t) = \frac{1}{2w}\,\hat{u}\left(t-\frac{n}{w}\right) \tag{A-13}$$

Using these results we finally have

$$v(t) = \sum_{n=-\infty}^{\infty} \frac{1}{2w}\,h'\left(\frac{n}{w},t\right)\,u\left(t-\frac{n}{w}\right) - \sum_{n=-\infty}^{\infty} \frac{1}{2w}\,\hat{h}'\left(\frac{n}{w},t\right)\,\hat{u}\left(t-\frac{n}{w}\right) \tag{A-14}$$

EXAMPLE

Consider the filter in Fig. 11 consisting of a cascade of a frequency shift Δf and a time delay δ. The corresponding frequency function is

$$H(jf,t) = A\,e^{-j2\pi f\delta}\begin{cases} e^{j(2\pi\Delta ft+\phi)} & f>0 \\ e^{-j(2\pi\Delta ft+\phi)} & f<0 \end{cases} \tag{A-15}$$

If we restrict the filter to a bandwidth w around f_c, we have

$$H'(jf,t) = A\,e^{-j2\pi f\delta}\left[\text{rect}\left(\frac{f-f_c}{w}\right)e^{j(2\pi\Delta ft+\phi)} + \text{rect}\left(\frac{f+f_c}{w}\right)e^{-j(2\pi\Delta ft+\phi)}\right] \tag{A-16}$$

The corresponding function in the time domain is

$$h'(y,t) = A2w\ \text{sinc}\ w(y-\delta)\cos\left[2\pi(f_c(y-\delta)+\Delta ft)+\phi\right] \tag{A-17}$$

In the same way

$$\hat{h}'(y,t) = A2w\ \text{sinc}\ w(y-\delta)\sin\left[2\pi(f_c(y-\delta)+\Delta ft)+\phi\right]. \tag{A-18}$$

APPENDIX B

Modulated Random Processes

We want to determine the conditions under which a random process of the type

$$a(t) = x_c(t) \cos kt - x_s(t) \sin kt \tag{B-1}$$

is (strict sense) stationary independently of the value of k.

For a strict-sense stationary process all moments are independent of time. We have the first-order moment of a(t).

$$E[a(t)] = E[x_c] \cos kt - E[x_s] \sin kt \tag{B-2}$$

The only way that we can get this to be a constant that is independent of time for every value of k is by setting

$$E[x_c] = E[x_s] = 0. \tag{B-3}$$

The second-order moment is

$$E[a^2] = E\left[x_c^2\right] \cos^2 kt - 2E[x_c x_s] \cos kt \cdot \sin kt + E\left[x_s^2\right] \sin^2 kt$$

and the only acceptable solution is

$$E\left[x_c^2\right] = E\left[x_s^2\right] = \sigma^2 \tag{B-4}$$

$$E[x_c x_s] = 0. \tag{B-5}$$

For the third moment we have

$$E[a^3] = E\left[x_c^3\right] \cos^3 kt - 3E\left[x_c^2 x_s\right] \cos^2 kt \cdot \sin kt + 3E\left[x_c x_s^2\right] \cos kt \sin^2 kt - E\left[x_s^3\right] \sin^3 kt \tag{B-6}$$

which gives

$$E\left[x_c^3\right] = E\left[x_c^2 x_s\right] = E\left[x_c x_s^2\right] = E\left[x_s^3\right] = 0. \tag{B-7}$$

For the fourth moment we obtain

$$E[a^4] = E\left[x_c^4\right] \cos^4 kt - 4E\left[x_c^3 x_s\right] \cos^3 kt \cdot \sin kt + 6E\left[x_c^2 x_s^2\right] \cos^2 kt \cdot \sin^2 kt - 4E\left[x_c x_s^3\right] \cos kt \cdot \sin^3 kt + E\left[x_s^4\right] \sin^4 kt \tag{B-8}$$

which gives

$$E\left[x_c^3 x_s\right] = E\left[x_c x_s^3\right] = 0 \tag{B-9}$$

$$E\left[x_c^4\right] = E\left[x_s^4\right] = 3E\left[x_c^2 x_s^2\right]. \tag{B-10}$$

If we continue this procedure we see that

$$E\left[x_c^\nu\right] = E\left[x_s^\nu\right] \qquad \nu = 1, 2, \ldots$$

and since all of the moments are equal, x_c and x_s must have the same distribution, and we can state the following condition: A necessary condition for a to be stationary is that x_c and x_s are uncorrelated, equally distributed random variables with zero mean. With the additional assumption that x_c and x_s are independent, Eq. B-10 becomes

$$E\left[x_c^4\right] = E\left[x_s^4\right] = 3\left(E\left[x_c^2\right]\right)^2 = 3\sigma^4 \tag{B-11}$$

and by computing higher order moments, with the assumptions that the moments of all orders exist, we obtain

$$E\left[x_s^n\right] \begin{cases} = 1 \cdot 3 \cdot 5 \ldots (n-1)\left[E\left[x_s^2\right]\right]^{n/2} & n \text{ even} \\ = 0 & n \text{ odd} \end{cases} \tag{B-12}$$

The characteristic function for x_s and x_c is, then,

$$M_x(j\nu) = \sum_{n=0}^{\infty} E[x^n]\frac{(j\nu)^n}{n!} = \sum_{m=0}^{\infty} \frac{(j\nu\sigma)^{2m}}{2^m m!} = \exp\left(-\frac{\nu^2\sigma^2}{2}\right) \tag{B-13}$$

which is the Gaussian distribution.

Correlation Functions

Thus far, we have only considered first-order statistics and the conditions given are only necessary to insure stationariness.

By expressing the correlation function of a(t) in terms of the correlation functions for $x_s(t)$ and $x_c(t)$, we can obtain other necessary conditions.

Assume that $x_c(t)$ and $x_s(t)$ are (wide sense) stationary processes with zero mean, so that we can write

$$R_c(\tau) = E[x_c(t+\tau)x_c(t)]$$

$$R_s(\tau) = E[x_s(t+\tau)x_s(t)]$$

$$R_{sc}(\tau) = E[x_s(t+\tau)x_c(t)]$$

$$R_{cs}(\tau) = E[x_c(t+\tau)x_s(t)].$$

The autocorrelation of a(t) is readily obtained.

$$R_a(t,\tau) = E[a(t+\tau)a(t)] = R_c(\tau)\cos k(t+\tau)\cdot\cos kt + R_s(\tau)\sin k(t+\tau)\sin kt$$

$$- R_{cs}(\tau)\cos k(t+\tau)\sin kt - R_{sc}(\tau)\sin k(t+\tau)\cos kt. \qquad \text{(B-15)}$$

For R_a to be a function of only τ we must have

$$R_c(\tau) = R_s(\tau)$$

$$R_{cs}(\tau) = -R_{sc}(\tau). \qquad \text{(B-16)}$$

Substituting these expressions in (B-15) gives

$$R_a(\tau) = R_c(\tau)\cos k\tau + R_{cs}\sin k\tau. \qquad \text{(B-17)}$$

Under these assumptions the correlation of the function

$$b(t) = x_c(t)\sin kt + x_s(t)\cos kt \qquad \text{(B-18)}$$

is the same as for a(t).

$$R_b(\tau) = R_c(\tau)\cos k\tau + R_{cs}\sin k\tau. \qquad \text{(B-19)}$$

The crosscorrelation between a(t) and b(t) is

$$R_{ab}(\tau) = R_{cs}(\tau)\cos k\tau - R_c(\tau)\sin k\tau$$

$$R_{ba}(\tau) = R_{cs}(\tau)\cos k\tau + R_c(\tau)\sin k\tau. \qquad \text{(B-20)}$$

We see that even if $x_s(t)$ and $x_c(t)$ are independent random processes (so that $R_{cs}(t) = R_{sc}(t) \doteq 0$), a(t) and b(t) are not independent.

APPENDIX C

Regression-Line Prediction

Assume that we have a wide-sense stationary process $y(t) = s(t) + n(t)$ sampled at distances δ apart. Call $N\delta = \tau$, where N is a positive integer. Under the time interval $-\tau$ to 0 we want to fit a straight line to y(t) so that

$$\psi(a, b) = \sum_{\nu=0}^{N} [y(-\nu\delta) - (a - b\nu\delta)]^2 \tag{C-1}$$

is minimum (see Fig. 23).

$$\left.\begin{aligned} \frac{\partial\psi}{\partial a} &= -2 \sum_{\nu=0}^{N} [y(-\nu\delta) - a + b\nu\delta] = 0 \\ \frac{\partial\psi}{\partial b} &= 2\delta \sum_{\nu=0}^{N} [y(-\nu\delta) - a + b\nu\delta] = 0 \end{aligned}\right\}$$

$$\left.\begin{aligned} \sum_{\nu=0}^{N} y(-\nu\delta) &= (N+1)\, a - b\delta \sum_{\nu=0}^{N} \nu \\ \sum_{\nu=0}^{N} \nu y(-\nu\delta) &= a \sum_{\nu=0}^{N} \nu - b\delta \sum_{\nu=0}^{N} \nu^2 \end{aligned}\right\}$$

Using the formulas

$$\sum_{0}^{N} \nu = \frac{N(N+1)}{2} \tag{C-2}$$

$$\sum_{0}^{N} \nu^2 = \frac{N(N+1)(2N+1)}{6}, \tag{C-3}$$

we obtain

$$a = \frac{2(2N+1)}{(N+1)(N+2)} \left[\sum_{\nu=0}^{N} y(-\nu\delta) - \frac{3}{2N+1} \sum_{\nu=0}^{N} \nu y(-\nu\delta) \right] \tag{C-4}$$

$$\delta b = \frac{6}{(N+1)(N+2)} \left[\sum_{\nu=0}^{N} y(-\nu\delta) - \frac{2}{N} \sum_{\nu=0}^{N} \nu y(-\nu\delta) \right]. \tag{C-5}$$

Mean-Square Error $\Lambda(T)$

The mean-square error with the regression line used as predictor is

$$\Lambda(T) = E[(s(T)-(a+bT))^2]$$

$$= E[s^2(T)+a^2+b^2T^2-2as(T)-2Tbs(T)+2Tab]. \qquad (C-6)$$

To evaluate $\Lambda(T)$, we substitute the expressions for a and b (C-4) and (C-5) in (C-6) and take the mean of each term separately. To simplify the calculations, we assume that s(t) and the noise n(t) are uncorrelated and that $E[n(t)] = 0$. This means that we can write the autocorrelation function of y(t) as

$$R_y(\tau) = R_s(\tau) + R_n(\tau).$$

Moreover, we assume that the noise is uncorrelated between samples

$$R_n(k\delta) \begin{cases} = \sigma_n^2 & k = 0 \\ & k = 1, 2, 3, \ldots . \\ = 0 & k \geq 1 \end{cases} \qquad (C-7)$$

Evaluation of $E[a^2]$

Let us consider the evaluation of the term $E[a^2]$ in $\Lambda(T)$. From (C-4)

$$E[a^2] = \left[\frac{2(2N+1)}{(N+1)(N+2)}\right]^2 \left[\sum_{\nu=0}^{N}\sum_{\mu=0}^{N} E[y(-\nu\delta)y(-\mu\delta)] - \frac{6}{2N+1}\sum_{\nu=0}^{N}\sum_{\mu=0}^{N} \nu E[y(-\nu\delta)y(-\mu\delta)] + \frac{9}{(2N+1)^2}\sum_{\nu=0}^{N}\sum_{\mu=0}^{N} \nu\mu E[y(-\nu\delta)y(-\mu\delta)]\right]. \qquad (C-8)$$

The double sum in the first term is equal to

$$\sum_{\nu=0}^{N}\sum_{\mu=0}^{N} E[y(-\nu\delta)y(-\mu\delta)] = \sum_{\nu}\sum_{\mu} R_y[(\nu-\mu)\delta] = \sum_{\nu}\sum_{\mu} R_s + \sum_{\nu}\sum_{\mu} R_n.$$

Since the noise is uncorrelated at different sample points, the last term becomes

$$\sum_{\nu=0}^{N}\sum_{\mu=0}^{N} R_n[(\nu-\mu)\delta] = (N+1)\,\sigma_n^2. \qquad (C-9)$$

To evaluate the first term, we expand $R_s(t)$ in a power series around zero:

$$R_s(t) = R_s(0) + \tfrac{1}{2}R_s''(0)\,t^2 + O(|t|^3). \qquad (C-10)$$

Since we have restricted ourselves to differentiable sample functions, there is no first-order term. $R_s''(0)$ is the second derivative at zero. The notation for the remainder means that

$$\lim_{t\to 0} \frac{O(t^3)}{t^3} = \text{constant.}$$

Using (C-10), we get

$$\sum_{\nu=0}^{N}\sum_{\mu=0}^{N} R_s[(\nu-\mu)\delta] = \sum_{\nu=0}^{N}\sum_{\mu=0}^{N} R_s(0) + \frac{R_s''(0)}{2}\sum_{\nu=0}^{N}\sum_{\mu=0}^{N}(\nu-\mu)^2 + \sum_{\nu=0}^{N}\sum_{\mu=0}^{N} O(|\nu-\mu|^3\delta^3). \tag{C-11}$$

The sum in the second term from (C-2) and (C-3) is

$$\sum_{\nu=0}^{N}\sum_{\mu=0}^{N}(\nu-\mu)^2 = \sum_{\nu}\sum_{\mu}(\nu^2+\mu^2-2\nu\mu) = \frac{N(N+1)^2(N+2)}{6}. \tag{C-12}$$

In the same way,

$$\sum\sum O(|\nu-\mu|^3\delta^3) = O(N^5\delta^3).$$

We obtain from these results

$$\sum_{\nu=0}^{N}\sum_{\mu=0}^{N} R_y[(\nu-\mu)\delta] = (N+1)^2 R_s(0) + \frac{N(N+1)^2(N+2)}{12}\delta^2 R_s''(0) + (N+1)\sigma_n^2 + O(N^5\delta^3). \tag{C-13}$$

To evaluate the second term of $E[a^2]$, we write

$$\sum_{\nu=0}^{N}\sum_{\mu=0}^{N} \nu R_s[(\nu-\mu)\delta] = \sum_{\nu}\sum_{\mu}\nu R_s(0) + \frac{R_s''(0)}{2}\delta^2\sum_{\nu}\sum_{\mu}\nu(\nu-\mu)^2 + \sum_{\nu}\sum_{\mu} O(\nu|\nu-\mu|^3\delta^3). \tag{C-14}$$

Using the formula

$$\sum \nu^3 = \frac{N^2(N+1)^2}{4} \tag{C-15}$$

together with (C-2) and (C-3), we obtain

$$\sum_{\nu=0}^{N}\sum_{\mu=0}^{N}\nu(\nu-\mu)^2 = \frac{N^2(N+1)^2(N+2)}{12} \tag{C-16}$$

which gives

$$\sum_{\nu=0}^{N}\sum_{\mu=0}^{N}\nu R_s[(\nu-\mu)\delta] = \frac{N(N+1)^2}{2}R_s(0) + \frac{N^2(N+1)^2(N+2)}{24}\delta^2 R_s''(0) + \frac{N(N+1)}{2}\sigma_n^2 + O(N^6\delta^3). \tag{C-17}$$

In a completely analogous way,

$$\sum\sum\nu\mu R_s[(\nu-\mu)\delta] = \frac{N^2(N+1)^2}{4}R_s(0) + \frac{(N-1)N^2(N+1)^2(N+2)}{72}\delta^2 R_s''(0) + \frac{N(N+1)(2N+1)}{6}\sigma_n^2 + O(N^7\delta^3). \tag{C-18}$$

By substituting (C-13), (C-17), and (C-18) in (C-8), we get

$$E[a^2] = R_s(0) - \frac{1}{6}(N-1)\,N\delta^2 R_s''(0) + \frac{2(2N+1)}{(N+1)(N+2)}\sigma_n^2 + O(N^3\delta^3). \tag{C-19}$$

Using the same technique, we obtain

$$E[b^2] = -R_s''(0) + \frac{12}{N(N+1)(N+2)}\frac{\sigma_n^2}{\delta^2} + O(N\delta) \tag{C-20}$$

$$E[ab] = -\frac{1}{2}N\delta R_s''(0) + \frac{6}{(N+1)(N+2)}\frac{\sigma_n^2}{\delta} + O(N\delta) \tag{C-21}$$

$$E[as(T)] = R_s(T) - \frac{1}{12}(N-1)\,N\delta^2 R_s''(T) + O(N^3\delta^3) \tag{C-22}$$

$$E[bs(T)] = -R_s'(T) - \frac{1}{2}N\delta R_s''(T) + O(N^2\delta^2). \tag{C-23}$$

Here, $R_s'(T)$ and $R_s''(T)$ are the first and second derivatives of $R_s(t)$ at $t = T$.

Substituting these terms in (C-6) and assuming that $N\delta = \tau$ is small enough yields

$$\Lambda(T) = 2\left[R(0) - R_s(T) - \frac{T^2}{2}R''(0) + TR'(T)\right] + (R_s''(T)\;\; R_s''(0))\left[T\tau + \frac{N-1}{6N}\tau^2\right] + \frac{4N\sigma_n^2}{(N+1)(N+2)}\left[3\frac{T^2}{\tau^2} + 3\frac{T}{\tau} + \frac{2N+1}{2N}\right]. \tag{C-24}$$

Introducing some new notation, we can write

$$\Lambda(T) = \Gamma(T) + \Psi(T)\left[\frac{\tau}{T} + \frac{N-1}{6N}\frac{\tau^2}{T^2}\right] + \frac{4}{N}\Phi(N)\sigma_n^2\left[3\frac{T^2}{\tau^2} + 3\frac{T}{\tau} + \frac{2N+1}{2N}\right], \tag{C-25}$$

where

$$\Gamma(T) = 2\left[R(0) - R_s(T) - \frac{T^2}{2}R''(0) + TR'(T)\right]$$

$$\Psi(T) = T^2(R_s''(T) - R_s''(0))$$

$$\Phi(N) = \frac{N^2}{(N+1)(N+2)} .$$

APPENDIX D

The Weighting Function W(U, V)

To study the properties of the weighting function W(U, V) in (114) we can equivalently consider the argument of the logarithm.

We want to prove certain properties of the function

$$F(U, V) = \int_{-\infty}^{\infty} \int_{-\infty}^{\infty} \exp\left\{\frac{E}{N_o}\left[2Ux+2Vy-x^2-y^2\right]\right\} p(x, y)\, dx\, dy, \tag{D-1}$$

where p(x, y) is a probability density function, and E and $N_o > 0$. Since all of the terms in the integral are greater than zero, we have

$$F(U, V) \geq 0 \qquad \text{for all } U, V.$$

The second derivative of F(U, V) with respect to V is

$$\frac{\partial^2 F}{\partial V^2} = \int_{-\infty}^{\infty} \int_{-\infty}^{\infty} \left(\frac{2Ey}{N_o}\right)^2 \exp\left\{\frac{E}{N_o}\left[2Ux+2Vy-x^2-y^2\right]\right\} p(x, y)\, dx\, dy \tag{D-2}$$

and we have

$$\frac{\partial^2 F}{\partial V^2} > 0$$

$$\frac{\partial^2 F}{\partial U^2} > 0 \qquad \text{for all } U, V.$$

By using the Schwartz inequality, it can also be shown that

$$\frac{\partial^2 F}{\partial V^2}\,\frac{\partial^2 F}{\partial U^2} - \left(\frac{\partial^2 F}{\partial U\, \partial V}\right)^2 > 0.$$

This implies that F(U, V) cannot have any saddle points. If it has a minimum, it is a true minimum, and the function is monotonically increasing in all directions from the minimum.

It is possible to prove the following theorem.

THEOREM D: A necessary and sufficient condition for F(U, V) to have a minimum at a finite point in the UV-plane is that p(x, y) is different from zero in more than half of the xy-plane. That is, it is not possible to draw a straight line through the origin in the xy-plane so that p(x, y) is identically zero on either side of the line.

PROOF D: First, we prove that the condition is necessary. If p(x, y) is zero in half of the xy-plane, we can rotate the xy coordinate system so that

$$p(x', y') = 0 \qquad \text{for } y' < 0$$

$$\left.\begin{aligned} x' &= x\cos\theta - y\sin\theta \\ y' &= x\sin\theta + y\cos\theta \end{aligned}\right\}. \tag{D-3}$$

By making the same rotation in the UV-plane,

$$\left.\begin{aligned} U' &= U\cos\theta - V\sin\theta \\ V' &= U\sin\theta + V\cos\theta \end{aligned}\right\}. \tag{D-4}$$

The integral (A-1) is not changing and, using the x'y' and U'V' coordinates, we have

$$\frac{\partial F}{\partial V'} = \int_{-\infty}^{\infty}\int_{0}^{\infty} \frac{2Ey'}{N_o} \exp\left\{\frac{E}{N_o}[2U'x'+2V'y'-x'^2-y'^2]\right\} p(x', y')\, dy'\, dx' \tag{D-5}$$

Since all terms in the inner integral are equal to or greater than zero for all values of x' we have

$$\frac{\partial F}{\partial V'} > 0 \qquad \text{for all } U', V'$$

and thus there is no finite point that is such that

$$\frac{\partial F}{\partial V'} = 0; \quad \frac{\partial F}{\partial U'} = 0$$

which is a necessary condition for a minimum.

Second, we prove that the condition is sufficient by showing that it is possible to draw a closed contour in the UV-plane so that the derivative in the direction of the radius vector is greater than zero,

$$\frac{\partial F}{\partial r} > 0,$$

for all points on the contour. Since the second derivatives are positive in all directions, there can be only one minimum inside the contour.

We compute $\left(\frac{\partial F}{\partial V}\right)_{U=0}$ for an arbitrary direction of the UV coordinate axis and choose the xy axis correspondingly

$$\left(\frac{\partial F}{\partial V}\right)_{U=0} = \int_{-\infty}^{\infty}\int_{-\infty}^{\infty} \frac{2Ey}{N_o} \exp\left\{\frac{E}{N_o}[2Vy-y^2]\right\}\exp\left(-\frac{E}{N_o}x^2\right) p(x, y)\, dx\, dy \tag{D-6}$$

We split the integral into two halves and after a change fo variable obtain

$$\begin{aligned}\left(\frac{\partial F}{\partial V}\right)_{U=0} &= \int_{-\infty}^{\infty} \exp\left(-\frac{E}{N_o}x^2\right) \int_{0}^{\infty} \frac{2Ey}{N_o} \exp\left\{\frac{E}{N_o}[2Vy-y^2]\right\} p_+(x, y)\, dy\, dx \\ &\quad - \int_{-\infty}^{\infty} \exp\left(-\frac{E}{N_o}x^2\right) \int_{0}^{\infty} \frac{2Ey}{N_o} \exp\left\{-\frac{E}{N_o}[2Vy+y^2]\right\} p_-(x, -y)\, dy\, dx \\ &= I_+(V) - I_-(V). \end{aligned} \tag{D-7}$$

Here, p_+ and p_- denote the probability density in the upper and lower half-planes, respectively.

Next, we split I_+ and I_- into two halves, integrating, first, over a strip of width 2δ around the x-axis. Let

$$A = \int_{-\infty}^{\infty} \exp\left\{-\frac{E}{N_o} x^2\right\} \int_0^{\delta} \frac{2Ey}{N_o} \exp\left\{\frac{E}{N_o}[2Vy-y^2]\right\} p_+(x,y)\, dy\, dx \qquad \text{(D-8)}$$

$$B = \int_{-\infty}^{\infty} \exp\left\{-\frac{E}{N_o} x^2\right\} \int_0^{\delta} \frac{2Ey}{N_o} \exp\left\{-\frac{E}{N_o}[2Vy+y^2]\right\} p_-(x,-y)\, dy\, dx \qquad \delta > 0. \quad \text{(D-9)}$$

Clearly, both A and B are greater than or equal to zero.

Since all terms in I_+ and I_- are positive, we can write

$$I_+(V) \geq A + \exp\left(\frac{2E}{N_o} V\delta\right) \int_{-\infty}^{\infty} \int_{\delta}^{\infty} \frac{2Ey}{N_o} \exp\left\{-\frac{E}{N_o}[x^2+y^2]\right\} p_+(x,y)\, dy\, dx \qquad \text{(D-10)}$$

$$I_-(V) \leq B + \exp\left(-\frac{2E}{N_o} V\delta\right) \int_{-\infty}^{\infty} \int_{\delta}^{\infty} \frac{2Ey}{N_o} \exp\left\{-\frac{E}{N_o}[x^2+y^2]\right\} p_-(x,-y)\, dy\, dx. \quad \text{(D-11)}$$

According to our assumptions p_+ or p_- are not identically zero and, as long as the whole probability mass is not located as impulses along the x-axis, we have

$$\left(\frac{\partial F}{\partial V}\right)_{U=0} = I_+(V) - I_-(V) \geq A + C \exp\left(\frac{2E}{N_o} V\delta\right) - B - D \exp\left(-\frac{2E}{N_o} V\delta\right)$$

$$(A, B, C, D \text{ and } \delta > 0) \qquad \text{(D-12)}$$

The fact that p(x, y) is a probability density ensures that all integrals involved in the proof converge.

Thus it is possible to find a $V = R_V > 0$ with the property that

$$\left(\frac{\partial F}{\partial V}\right)_{U=0,\, V=R_V} > 0. \qquad \text{(D-13)}$$

Since we have proved this for an arbitrary orientation of the coordinate system, we can find such an R_V in all directions, and that completes the proof.

Acknowledgment

I am particularly indebted to Professor John M. Wozencraft, who suggested my thesis problem, for his encouragement and guidance through the work.

I wish to thank Professor Edward M. Hofstetter and Professor William M. Siebert for helpful conversations, and my fellow-student James L. Massey for help with proofreading the manuscript.

I am grateful to William B. Smith and Martin Balser of Lincoln Laboratory, M.I.T., for supplying the ionospheric data used in Section III.

I also wish to express my appreciation to the Research Laboratory of Electronics, M.I.T., for making this research possible and to the Computation Center, M.I.T., for use of the IBM 709 computer.

References

1. D. K. Bailey, R. Bateman, L. V. Berkner, H. G. Booker, G. F. Montgomery, E. M. Purcell, W. W. Salisbury, and J. B. Wiesner, A new kind of radio propagation at very high frequencies observable over long distances, Phys. Rev. 86, 141-145 (1952).
2. M. Balser, W. B. Smith, and E. Warren, On the reciprocity of HF ionospheric transmission, J. Geophys. Res. 63, 859 (1958).
3. H. G. Booker and W. E. Gordon, A theory of radio scattering in the troposphere, Proc. IRE 38, 401 (1950).
4. D. G. Brennan and M. L. Phillips, Phase and Amplitude Variability in Medium-Frequency Ionospheric Transmission, Technical Report No. 93, Lincoln Laboratory, M.I.T., September 16, 1957.
5. D. G. Brennan, Linear diversity combining techniques, Proc. IRE 47, 1075 (1959).
6. K. G. Budden, Radio Waves in the Ionosphere (Cambridge University Press, London, 1961).
7. W. B. Davenport and W. L. Root, An Introduction to the Theory of Random Signals and Noise (McGraw-Hill Book Company, New York, 1958); see especially Chapter 8.
8. J. L. Doob, Stochastic Processes (John Wiley and Sons, Inc., New York, 1953).
9. R. M. Fano, Transmission of Information (The M.I.T. Press, Cambridge, Mass., and John Wiley and Sons, Inc., New York, 1961); see especially Chapter 6.
10. C. W. Helstrom, Statistical Theory of Signal Detection (Pergamon Press, London, 1960); see especially Chapters IV and V.
11. T. Kailath, Correlation detection of signals perturbed by a random channel, Trans. IRE, Vol. IT-6, No. 3, June 1960.
12. T. Kailath, Channel Characterization: Time-Variant Dispersive Channels, Lectures on Communication System Theory, edited by E. J. Baghdady (McGraw-Hill Book Company, New York, 1961), Chapter 6.
13. Y. W. Lee, Statistical Theory of Communication (John Wiley and Sons, Inc., New York, 1960); see especially p. 13.
14. D. H. Pratt, Measurements of Magneto-Ionic Phase Stability, E.E. Thesis, Department of Electrical Engineering, M.I.T., September 1960.
15. R. Price, Statistical Theory Applied to Communication Through Multipath Disturbances, Technical Report No. 34, Lincoln Laboratory, M.I.T., September 3, 1953.
16. R. Price, Optimum detection of random signals in noise with application to scatter multipath communication, I., Trans. IRE, Vol. IT-2, No. 4, December 1956.
17. R. Price and P. E. Green, Communication technique for multipath channels, Proc. IRE 46, 555 (1958).
18. J. A. Ratcliffe, Diffraction from the Ionosphere and the Fading of Radio Waves, Nature 162, 9 (July 1948).
19. S. O. Rice, Mathematical analysis of random noise, Bell System Tech. J. 23, 282 (1944); 24, 46 (1945).
20. G. Turin, Communication Through Noisy, Random-Multipath Channels, Technical Report No. 116, Lincoln Laboratory, M.I.T., May 14, 1954.
21. G. Turin, Communication through noisy, random-multipath channels, IRE Convention Record, Part 4, 1956, p. 154.
22. G. Turin, Error probabilities for binary symmetric ideal reception through non-selective slow fading and noise, Proc. IRE 46, 1603 (1958).
23. F. Villars and V. F. Weisskopf, The scattering of electromagnetic waves by turbulent atmospheric fluctuations, Phys. Rev. 94, 232 (1954).

24. P. M. Woodward, Probability and Information Theory, with Applications to Radar (McGraw-Hill Book Company, New York, 1957).

25. J. L. Doob, op. cit., p. 537.

26. Ibid., p. 233.

27. W. B. Davenport and W. L. Root, op. cit.; see Chapter 11.